REES, B. (1977). *Isr. J. Chem.* **16**, 180–186.
SCHWARZENBACH, D., ABRAHAMS, S. C., FLACK, H. D., GONSCHOREK, W., HAHN, TH., HUML, K., MARSH, R. E., PRINCE, E., ROBERTSON, B. E., ROLLETT, J. S. & WILSON, A. J. C. (1989). *Acta Cryst.* A**45**, 63–75.
SHARMA, D. (1965). *Acta Cryst.* **18**, 818–819.
THOMAS, J. O., TELLGREN, R. & OLOVSSON, I. (1974). *Acta Cryst.* B**30**, 2540–2549.
WALDECK, W. F., LYNN, G. & HILL, A. E. (1934). *J. Am. Chem. Soc.* **56**, 43–47.
WILLIS, B. T. M. & PRYOR, A. W. (1975). *Thermal Vibrations in Crystallography*, p. 132. London: Cambridge Univ. Press.

Acta Cryst. (1990). B**46**, 474–487

Structure Refinement of Commensurately Modulated Bismuth Titanate, $Bi_4Ti_3O_{12}$

BY A. DAVID RAE

School of Chemistry, University of New South Wales, PO Box 1, *Kensington, New South Wales* 2033, *Australia*

AND JOHN G. THOMPSON, RAY L. WITHERS AND ANTHONY C. WILLIS

Research School of Chemistry, Australian National University, PO Box 4, *Canberra City* 2601, *Australia*

(*Received* 2 *November* 1989; *accepted* 2 *March* 1990)

Abstract

The displacive ferroelectric $Bi_4Ti_3O_{12}$ [M_r = 1171·6, a = 5·450 (1), b = 5·4059 (6), c = 32·832 (3) Å, β = 90·00°, Z = 4, D_x = 8·045 g cm^{-3}, Mo $K\alpha$, λ = 0·7107 Å, μ = 747·3 cm^{-1}, $F(000)$ = 1976] is described at room temperature as a commensurate modulation of an *Fmmm* parent structure derived from an idealized *I*4/*mmm* structure. Displacive modes of inherent *F*2*mm*, *Bmab* and *Bbab* symmetry are all substantial and reduce the space-group symmetry to *B*2*ab*. A further substantial displacive mode of *Bbam* symmetry reduces the space-group symmetry to *B*1*a*1 and induces minor displacive modes of *Fmm*2, *F*12/*m*1 and *Bmam* symmetry. A group-theoretical analysis of the problem details how the X-ray data can be classified so as to monitor the refinement. To a first-order approximation, the *F*2*mm* and *Bbab* symmetry components of atom displacements contribute only to the imaginary part of the structure factors. Because the structure factors have a predominant real component, it is easy to get the *F*2*mm* and *Bbab* displacive components of the O atoms wrong. False minima occur at values of 0·027 for $R_1 = \sum_{\mathbf{h}}||F_{obs}(\mathbf{h})| - |F_{calc}(\mathbf{h})||/\sum_{\mathbf{h}}|F_{obs}(\mathbf{h})|$ but a corrrect solution was obtained with R_1 = 0·0177 for 2839 unmerged data with $I(\mathbf{h}) > 2\sigma[I(\mathbf{h})]$. Criteria for a correct solution are evaluated and subsequently met. The final refinement used a 0·63:0·37 twin model.

Introduction

Within the family of so called Aurivillius phases (Aurivillius, 1949, 1950), there exists a large number of displacive ferroelectrics (Subbarao, 1973; Singh, Bopardikar & Atkare, 1988). These displacive ferroelectrics have room-temperature structures which can be described in terms of small displacive perturbations away from an *I*4/*mmm*, $a' = b'$ = 3·85 Å, prototype parent structure that consists of perovskite-like $A_{n-1}B_nO_{3n+1}$ slabs regularly interleaved with Bi_2O_2 layers (see Fig. 1 for n = 3). The parent structure is presumed to correspond to the crystal structure above the high-temperature phase transition which occurs at the so called Curie temperature. However, in several instances additional phase transitions are known to occur at different temperatures (Subbarao, 1973; Newnham, Wolfe & Dorrian, 1971). This poses questions as to the nature of these changes.

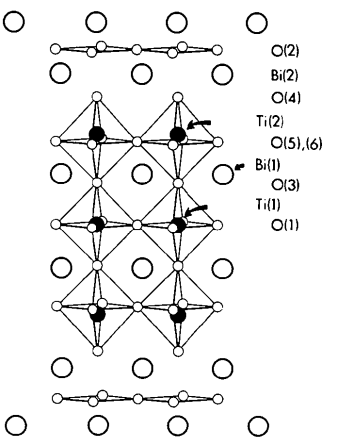

Fig. 1. A perspective drawing, approximately down ⟨110⟩, of the undistorted *Fmmm* parent structure of $Bi_4Ti_3O_{12}$. Only atoms between $\frac{1}{4}\mathbf{c}$ and $\frac{3}{4}\mathbf{c}$ are shown.

0108-7681/90/040474-14$03.00

Careful analysis of the diffraction patterns of a wide range of Aurivillius phases has revealed certain consistencies. From our work (Table 5), $Bi_2BaNb_2O_9$ appears to be the *I*4/*mmm* parent structure while $Bi_2SrNb_2O_9$, $Bi_2SrTa_2O_9$, $Bi_2BaTa_2O_9$ appear to have space group $A2_1am$. $Bi_3(Ti,Nb)O_9$ (Wolfe, Newnham, Smith & Kay, 1971) and $(Sr,Ba)BiTa_2O_9$ (Newnham, Wolfe, Horsey, Diaz-Colon & Kay, 1973) also appear to have space group $A2_1am$. However, Bi_2WO_6 (Wolfe, Newnham & Kay, 1969) and $Bi_4Ti_3O_{12}$ (Dorrian, Newnham, Smith & Kay, 1971) are reported to have space group *B*2*cb*. The **a** and **b** axes of the *A*- and *B*-centred lattices correspond to the diagonals $\mathbf{a}' \pm \mathbf{b}'$ of the parent structure. The choice between *A* or *B* centring is made so that the polar direction corresponds to **a**. One is tempted to conclude that when *n* is even the dominant displacive modes result in $A2_1am$ whereas when *n* is odd the dominant displacive modes result in *B*2*cb*. When no displacement occurs the structure remains as *I*4/*mmm*.

It should be noted that the space group with symmetry elements common to $A2_1am$ and *B*2*cb* is $P2_1ab$. Two symmetry elements (2_1 axis $\frac{1}{2}+x, -y, \frac{1}{2}-z$ and *b* glide $x, \frac{1}{2}+y, \frac{1}{2}-z$) describe symmetry across the Bi_2O_2 layers at $z = \pm\frac{1}{4}$ while the *a* glide $\frac{1}{2}+x, \frac{1}{2}-y, z$ relates atoms of the same *z* coordinate. The centring imposes relationships across the middle of the perovskite slab (2_1 axis $\frac{1}{2}+x, \frac{1}{2}-y, -z$ and mirror $x, y, -z$) for the *A*-centred (*n* even) case and (2 axis $x, -y, -z$ and *n* glide $\frac{1}{2}+x, \frac{1}{2}+y, -z$) for the *B*-centred (*n* odd) case.

Symmetry labels only contain sufficient information to generate all the equivalent positions. For example, because of the *B* centring, *B*2*cb* has 2: $x, -y, -z$ and 2_1: $\frac{1}{2}+x, -y, \frac{1}{2}-z$ parallel to **a**; *c*: $x, \frac{1}{2}-y, \frac{1}{2}+z$ and *a*: $\frac{1}{2}+x, \frac{1}{2}-y, z$ perpendicular to **b**; *b*: $x, \frac{1}{2}+y, \frac{1}{2}-z$ and *n*: $\frac{1}{2}+x, \frac{1}{2}+y, -z$ perpendicular to **c**. We have chosen labelling that emphasizes an *a* glide perpendicular to **b** as this is the symmetry element of $P2_1ab$ that is most relevant to atoms within a perovskite slab and we will henceforth refer to *B*2*ab* rather than *B*2*cb*.

However, $Bi_4Ti_3O_{12}$ is actually monoclinic as suggested by optical measurements (Dorrian *et al.*, 1971). Our electron diffraction experiments show that the true space group is *B*1*a*1 and not *B*2*ab* as the *b*-glide absences ($h = 2n$, $k = 2n+1$, $l = 0$) are weakly observed (Withers, Thompson, Wallenberg, FitzGerald, Anderson & Hyde, 1988). One concludes that there are a number of simultaneously existing modulation waves of different irreducible representations. It was decided to carefully collect and refine data for $Bi_4Ti_3O_{12}$ to check the validity of a previous analysis which imposed *B*2*ab* symmetry (Dorrian *et al.*, 1971). We found that many features of this structure are incorrect and this casts serious doubts on the reported structure of $Bi_3(Ti,Nb)O_9$ (Wolfe *et al.*, 1971), which we will investigate in another paper.

*B*1*a*1 can be transformed to *P*1*c*1 using new axes $(\mathbf{a}+\mathbf{c})/2$, **b**, **c** and the origin relocated to put the glide at $y = 0$. However, these modifications only hinder the understanding of the structure. Since *B*1*a*1 and *B*2*ab* are subgroups of *Fmmm* with the same **a**, **b**, **c** axes we consider it preferable to use the origin and axis choice which leaves equivalent positions unchanged.

Group-theoretical considerations

Modulated structures may be described in terms of occupancy and displacive waves associated with points of a Brillouin zone in reciprocal space. These waves describe changes in atomic parameters and linear combinations of atomic parameters away from those implied by the higher symmetry of a parent structure. The parent structure should be regarded as an idealized structure and it is not necessary that the parent structure should exist under some physical conditions in order that an actual structure be regarded as modulated. Nevertheless $Bi_4Ti_3O_{12}$ does exist as a tetragonal structure above 948 K (Newnham *et al.*, 1971). Distortions of the crystal lattice can be an independent aspect of the description if we regard symmetry operations as acting on scattering density described using fractional coordinates. Loss of symmetry allows the lattice distortion.

We can describe single-atom parameters of the modulated structure using the parent structure for reference. The *r*th single-atom variable parameter associated with the *q*th equivalent position of the *n*th atom in the reference asymmetric unit of the parent structure may be described as

$$v_{nqr} = v_{nqro} + \Delta v_{nqr}$$

where Δv_{nqr} is the change of the parameter away from the value v_{nqro} which would hold if the symmetry of the parent structure were maintained.

Symmetrized parameters s_{npr} can substitute for the single-atom parameters where $\Delta s_{npr} = \sum_q A_{pq} \Delta v_{nqr}$ so that $\Delta v_{nq'r} = \sum_p B_{q'p} \Delta s_{npr}$, where $\sum_p B_{q'p} A_{pq} = \delta_{q'q}$ and $\delta_{q'q}$ are elements of the indentity matrix.

Parameter changes Δs_{npr} and Δv_{nqr} span exactly the same variable space, and structure refinement can be considered equally well in either parameter system since

$$\partial F(hkl)/\partial s_{npr} = \sum_q B_{qp} \partial F(hkl)/\partial v_{nqr}.$$

Group theory (Bradley & Cracknell, 1972) may be used to select sensible coefficients A_{pq} from the irreducible representations $\Gamma^{\mu}(\mathbf{R}_q)_{ij}$ of the space group. These coefficients can be chosen as particular matrix elements (*p* corresponding to particular

choices of μ, i, j) of irreducible representations so as to be independent of r and n. This requires that the parameters for any particular asymmetric unit of the parent group be defined relative to an axial system related to a reference axial system by the symmetry element used to create the asymmetric unit. The coefficients can be subsequently modified by changing axial systems.

The subscript q runs over equivalent positions in all the unit cells of the parent structure. $\Gamma^{\mu}(\mathbf{R}_q)_{ij}$ is the ij element of the μth irreducible representation of dimensions N_μ for $\mathbf{R}_q$, the qth of $N = N_s N_c$ symmetry elements $\mathbf{R}_q = (\mathbf{T}_q, \mathbf{t}_q)$ that shift $\mathbf{r}$ to $\mathbf{T}_q\mathbf{r} + \mathbf{t}_q$. N_s is the number of equivalent positions per unit cell and N_c is the number of unit cells of the parent structure. $\mathbf{T}_q$ is a point-symmetry operator and $\mathbf{t}_q$ is the associated translation. The $\mathbf{R}_q$ are the symmetry elements of the parent structure with scattering density $\rho(\mathbf{r})_o$ corresponding to $F(\mathbf{h})_o$.

Constraints on the refinement consist of setting specific Δs_{npr} to be identically zero, *i.e.* certain relationships $\sum_q A_{pq}\Delta v_{nqr} = 0$ hold betweeen changes Δv_{nqr} in standard atomic parameters. Some of these (p specific) may be necessarily imposed as a consequence of the modulated structure maintaining certain symmetry elements of the parent structure while others (n specific) may be necessarily imposed as a consequence of atoms having been on special positions in the parent group model. There remains the possibility of imposing constraints simply to assist refinement. In this context the use of certain symmetry elements of the parent group to impose constraints on relationships between thermal parameters of atoms no longer related by the symmetry of the modulated structure seems physically reasonable.

The group theory of the parent crystal structure creates irreducible representations associated with points $\mathbf{k}$ on a grid in the Brillouin zone of the crystal. If the μth irreducible representation is associated with the point $\mathbf{k}$ then $\Gamma^{\mu}(\mathbf{R}_{q'})_{ij} = \exp(-i\mathbf{k}.\mathbf{t}_{q'})D^{\mu}(\mathbf{T}_{q'})_{ij}$ for the subgroup $\{\mathbf{R}_{q'}\}$ of symmetry operations $\{\mathbf{R}_q = \mathbf{R}_{q'}\mathbf{R}_{q''}\}$ for which $\mathbf{T}_{q'}\mathbf{k} = \mathbf{k} + \mathbf{g}$ where $\mathbf{g}$ is a Bragg reflection of the parent group, see Bradley & Cracknell (1972, chapter 5). Points on the star of $\mathbf{k}$, *i.e.* the points $\mathbf{T}_{q''}\mathbf{k}$, have equivalent sets of matrices $D^{\mu}(\mathbf{T}_{q'})_{ij}$.

For a commensurately modulated structure there are only a finite number of values of $\exp(-i\mathbf{k}.\mathbf{t}_{q'})$ compared with an infinite number for an incommensurately modulated structure. Thus a commensurately modulated structure has an identifiable translationally repeating lattice and a primitive cell volume that is an integral multiple of the primitive cell volume of the parent structure.

Although such a structure is capable of being refined as an unmodulated structure, there are advantages in using the commensurately modulated approach, especially when trying to understand problems in refinement.

For pseudosymmetric or modulated structures we can use the irreducible representations for the symmetry operators of a parent structure and say that the scattering density $\rho(\mathbf{r}) = \sum_p \rho_p(\mathbf{r})$ where $\rho_p(\mathbf{r})$ is the pth symmetrized component of the scattering density. $\rho_p(\mathbf{r}) = \sum_q A_{pq}\rho(\mathbf{R}_q\mathbf{r})/N_p$ and $N_p = \sum_q |A_{pq}|^2$. $F(\mathbf{h}) = \sum_p F_p(\mathbf{h})$ where $F_p(\mathbf{h})$ is the Fourier transform of $\rho_p(\mathbf{r})$. The orthogonality of irreducible representations gives

$$\sum_q |F(\mathbf{T}_q^{-1}\mathbf{h})|^2/N_q = \sum_p |F_p(\mathbf{h})|^2$$

where $F_p(\mathbf{h}) = \sum'_q \exp(i\mathbf{h}.\mathbf{t}_q)A_{pq}F(\mathbf{T}_q^{-1}\mathbf{h})/N_p$. For a particular $\mathbf{h}$ the summations are only over those selections of p (choice of μ, i, j and hence $\mathbf{k}$) and q for which $\mathbf{T}_q^{-1}\mathbf{h} = \mathbf{g} + \mathbf{k}$. N_q is the number of pseudoequivalent reflections with intensities $|F(\mathbf{T}_q^{-1}\mathbf{h})|^2$. Other points on the star of $\mathbf{k}$ have been excluded.

In the case of $Bi_4Ti_3O_{12}$, $\mathbf{T}_q^{-1}\mathbf{h} = \mathbf{g} + \mathbf{k}$ holds for all symmetry operations of the parent structure of *Fmmm* symmetry when considering the Brillouin-zone points $\mathbf{k} = 0$ and $\mathbf{k} = \mathbf{a}^*$. Eight irreducible representations are possible for each point but only two of those at each point may be used to describe modulations within the constraint of *B*2*ab* symmetry. A further two at each point may be used when the symmetry is reduced to *B*1*a*1.

For the *B*2*ab* constraint $[|F(\mathbf{h})|^2 + |F(-\mathbf{h})|^2]/2 = \sum_p |F_p(\mathbf{h})|^2$ for calculated models and for any observed $F(\mathbf{h})$ the values of $F_p(\mathbf{h})$ are nonzero for only two values of p. Relative phases for the $F_p(\mathbf{h})$ components select the origin and polarity (four degrees of freedom) of the structure. For anomalous scattering the difference between $|F(\mathbf{h})|$ and $|F(-\mathbf{h})|$ permits a correct choice of polarity. The phases of the extra $F_p(\mathbf{h})$ components associated with *B*1*a*1 are determined by differences in magnitudes of the real and imaginary components of pseudoequivalent reflections. This allows refinement of atom parameters away from values imposing *B*2*ab* symmetry. If the observed differences in intensity of pseudoequivalent reflections are reduced by twinning then refinement problems can be expected. Problems can also be expected when certain $F_p(\mathbf{h})$ components dominate the data.

Restricting ourselves to nonglobal parameters (*i.e.* excluding scale, extinction *etc.*) we can use a Taylor expansion to describe the structure factor as

$$F(\mathbf{h}) = F(\mathbf{h})_o + \sum_n \sum_{pr} [\partial F(\mathbf{h})/\partial s_{npr}]_o \Delta s_{npr} + \tfrac{1}{2}\sum_n \sum_{prp'r'} [\partial^2 F(\mathbf{h})/\partial s_{npr}\partial s_{np'r'}]_o \Delta s_{npr}\Delta s_{np'r'} + \ldots$$

where the subscript o implies evaluation using the parameters associated with the parent structure. If the only variables are occupancy parameters ($r = 1$, say) and $\rho(\mathbf{r})_o$ corresponds to the $p = 1$ irreducible

representation in which all A_{1q} equal 1, then the above series expansion terminates after the first-order terms and for other p values, $F_p(\mathbf{h}) = \sum_n[\partial F(\mathbf{h})/\partial s_{np1}]_o \Delta s_{np1}$.

If the only variables are for displacements of atom positions then the series is infinite as we are differentiating $\exp(i\mathbf{h}.\mathbf{r})$-type terms and the symmetry of terms in Δs_{npr}, $\Delta s_{npr}\Delta s_{np'r'}$, *etc.* determines which $F_p(\mathbf{h})$ component is contributed to by which particular term in the series expansion. In particular, if p and p' are associated with Brillouin-zone points $\mathbf{k}$ and $\mathbf{k}'$ then the $\Delta s_{npr}\Delta s_{np'r'}$ term is associated with a contribution for the point $\mathbf{k} + \mathbf{k}'$.

Provided displacements are sufficiently small the first-order terms in the series are dominant and certain parameter combinations Δs_{npr} are determined by certain components of the data since $F_p(\mathbf{h})$ is approximated by $\sum_{nr}[\partial F(\mathbf{h})/\partial s_{npr}]_o \Delta s_{npr}$. The apparent scale of $F_p(\mathbf{h})$ data and hence Δs_{npr} parameters may be altered by disorder and twinning.

In the case of $Bi_4Ti_3O_{12}$, refinement used standard atom parameters in a standard manner but results and reflection data were analysed using a modulated structure approach. The only constraints were to maintain *B2ab* symmetry for the anisotropic thermal parameters of atoms pseudorelated by this symmetry. The only additional parameterization was a twinning parameter.

$Bi_4Ti_3O_{12}$ and other Aurivillius phases may be described using displacements of atoms away from higher symmetry positions in an *I4/mmm* symmetry parent structure. Displacements can be considered in two parts. There is a distortion of the crystal lattice without change of fractional coordinates in the unit cell and there is also the change in fractional coordinates. In all likelihood the distortion of the lattice is a consequence of the symmetry lowering of the fractional coordinate displacements. $Bi_4Ti_3O_{12}$ (along with a number of other Aurivillius phases) forms a structure with a *B*- (or *A*-) centred lattice and has $a \neq b$. A transformation can be made so that the tertiary $\mathbf{a}' + \mathbf{b}'$ and $\mathbf{a}' - \mathbf{b}'$ directions of *I4/mmm* become the **a**- and **b**-axis directions of *F4/mmm* and transformed fractional coordinates can be calculated. The lattice distortion reduces the lattice symmetry to *Fmmm*. 90° twinning is observed and corresponds to the freezing in locally of either one or the other of two equal energy structures. The observed *B*-centred structure is a consequence of modulations corresponding to reciprocal space vectors $\mathbf{k} = 0$ and $\mathbf{k} = \mathbf{a}^*$ (or $\mathbf{k} = 0$ and $\mathbf{k} = \mathbf{b}^*$ for the *A*-centred equivalent structure). $\mathbf{a}^*$ and $\mathbf{b}^*$ are defined relative to the axes of *Fmmm*.

The *Fmmm* parent structure has atoms on special positions. The symmetries of the relevant special positions in *Fmmm* are 0,0,*z* 8(*i*) *mm*2; 0,0,$\frac{1}{2}$ 4(*b*) *mmm*; $\frac{1}{4},\frac{1}{4},z$ 16(*j*) 2_z; $\frac{1}{4},\frac{1}{4},0$ 8(*e*) $2/m_z$; $\frac{1}{4},\frac{1}{4},\frac{1}{4}$ 8(*f*) 222.

For the purpose of developing a logical argument to describe the likely modulations we shall discuss primarily an *A*-centred lattice, with an implied transformation to a *B*-centred lattice (swap *a* and *b*, *x* and *y*, *h* and *k*). Comparison with previous work is most easily understood if we prefer the **a** direction to the **b** direction as the major polar direction in the crystal.

We define $\mathbf{R}_q = (\mathbf{T}_q, \mathbf{t}_q)$ to be a symmetry operation where $\mathbf{R}_q\mathbf{r} = \mathbf{T}_q\mathbf{r} + \mathbf{t}_q$. *Fmmm* can be described as an abelian group of 16 symmetry operations modulo an *A*-centred lattice. Singly degenerate irreducible representations (p = 1–16) can be formed with characters $\chi_p(\mathbf{R}_q) = \pm 1$. Operations related by *A*-centred lattice translations have the same value of $\chi_p(\mathbf{R}_q)$. The *Fmmm* parent corresponds to the $p = 1$ irreducible representation for which all $\chi_p(\mathbf{R}_q) = +1$. All other irreducible representations (p = 2–16) have half the $\chi_p(\mathbf{R}_q)$ values +1 and half −1. If modulations corresponding to two or more of the irreducible representations coexist then the space group describing the overall symmetry contains only those operations for which $\chi_p(\mathbf{R}_q) = +1$ for each of the coexisting modulations. In particular if we consider modulations for the $p = 1$ irreducible representation and just one other irreducible representation then the resultant symmetry can be used as a label for an irreducible representation that is more informative than saying the *p*th tabulated one. This notation has been used before, for example by McConnell & Heine (1984).

The scattering density component $\rho_p(R)$ is antisymmetric with respect to symmetry operations for which $\chi_p(\mathbf{R}_q) = -1$ provided anomalous dispersion is ignored. As a consequence the contribution $F_p(\mathbf{h})$ of $\rho_p(\mathbf{r})$ to the structure factor is restricted in both phase and *hkl* index condition.

There are eight irreducible representations associated with $\mathbf{k} = 0$, *i.e.* $F_p(\mathbf{h})$ only contributes to *hkl ooo* or *eee* (*o* = odd, *e* = even), namely

Fmmm, *F*2/*m*11, *F*12/*m*1, *F*112/*m*
(structure-factor contribution *real*)

*F*222, *F*2*mm*, *Fm*2*m*, *Fmm*2
(contribution *imaginary*)

and eight associated with $\mathbf{k} = \mathbf{b}^*$, *i.e.* $F_p(\mathbf{h})$ only contributes to *hkl eoo* or *oee*, namely†

Ammm, *Amaa*, *Abma*, *Abam*
(structure-factor contribution *real*)

Abaa, *Abmm*, *Amam*, *Amma*
(contribution *imaginary*).

As a first approximation for refinement of a structure we shall consider the possibilities that create an *A*-centred space group containing eight symmetry

† The centre of inversion is at 0,0,0 for the first four and at $\frac{1}{4},\frac{1}{4},0$ for the final four representations. The irreducible representations associated with $\mathbf{k} = 0$, $\mathbf{k} = \mathbf{a}^*$, $\mathbf{k} = \mathbf{b}^*$ are listed in Table 1.

Table 1. *The irreducible representations of Fmmm associated with the* $\mathbf{k} = \mathbf{a}^*$, $\mathbf{k} = \mathbf{b}^*$, $\mathbf{k} = 0$ *points of the Brillouin zone and their effective space-group labels (see text)*

Only the symmetry elements with a zero translational component are listed.

	1	2_x	2_y	2_z	-1	m_x	m_y	m_z	$\mathbf{k} = \mathbf{a}^*$	$\mathbf{k} = \mathbf{b}^*$	$\mathbf{k} = 0$
X_1	+1	+1	+1	+1	+1	+1	+1	+1	*Ammm*	*Bmmm*	*Fmmm*
X_2	+1	+1	−1	−1	+1	+1	−1	−1	*Amaa*	*Bmab*	*F2/m11*
X_3	+1	−1	−1	+1	+1	−1	−1	+1	*Abam*	*Bbam*	*F112/m*
X_4	+1	−1	+1	−1	+1	−1	+1	−1	*Abma*	*Bbmb*	*F12/m1*
X_5	+1	+1	+1	+1	−1	−1	−1	−1	*Abaa*	*Bbab*	*F222*
X_6	+1	+1	−1	−1	−1	−1	+1	+1	*Abmm*	*Bbmm*	*F2mm*
X_7	+1	−1	−1	+1	−1	+1	+1	−1	*Amma*	*Bmmb*	*Fmm2*
X_8	+1	−1	+1	−1	−1	+1	−1	+1	*Amam*	*Bmam*	*Fm2m*

elements per centred cell, *i.e.* four symmetry elements per primitive cell. Each space group corresponds to the common subgroup of two centrosymmetric *A*-centred orthorhombic space groups. Two pseudosymmetry generators $\mathbf{R}_1$ and $\mathbf{R}_2$ can be used to select four irreducible representations of *Fmmm*, namely *A* with $\chi_1(\mathbf{R}_1) = \chi_1(\mathbf{R}_2) = 1$ corresponding to *Fmmm*, B_1 with $\chi_2(\mathbf{R}_1) = 1$, $\chi_2(\mathbf{R}_2) = -1$ and B_2 with $\chi_3(\mathbf{R}_1) = -1$, $\chi_3(\mathbf{R}_2) = 1$ corresponding to two centrosymmetric *A*-centred orthorhombic space groups whose common subgroup is the possible space group, and B_3 with $\chi_4(\mathbf{R}_1) = \chi_4(\mathbf{R}_2) = -1$ corresponding to an implied *F*-centred space group. The implied symmetry can be obtained by multiplying the characters of the irreducible representatives in Table 1. For example *Abma* and *Amma* imply *F2mm*, *i.e.* X_4 and X_7 imply X_6. The common subgroup is centrosymmetric and monoclinic when B_1 and B_2 correspond to *A*-centred space groups with coincident centres of inversion, but noncentrosymmetric and orthorhombic otherwise. The symmetrized components $F_p(\mathbf{h})$ of $F(\mathbf{h})$ may be described as $[F(\mathbf{h}) \pm F(\mathbf{Th})]/2$ where **h** and **Th** are pseudosymmetrically related reflections. Twinning must always be considered as a possibility.

In Table 2 we have shown how displacements from points of higher symmetry in *Fmmm* transform. Two special positions are considered: (1) 0,0,*z* 8(*i*) *mm2* and (2) $\frac{1}{4},\frac{1}{4},z$ 16(*j*) 2_z. The other possible special positions relevant to Aurivillius phases (see above) select the value of *z* to coalesce pairs of equivalent special positions. Only equivalent positions describing atoms between $\frac{1}{4}$ and $\frac{3}{4}$ are listed. Either *A*- or *B*-centring relates these atoms to those between $\pm\frac{1}{4}$ but this simply imposes an index condition ($k + l = 2n$ only or $h + l = 2n$ only) on observed reflections. Contributions to structure factors for small displacements are categorized by the *h* and *k* indices. Different displacive modes have totally different functional forms for the displacements and elaborate the essential orthogonality of different $F_p(\mathbf{h})$ components.

The segmentation of structural information by *h* and *k* index is noteworthy. Table 3 selects from Table 2 the information specific to those irreducible representations for which the characters are +1 in either $A2_1am$ and *B2ab*, the space groups assumed for a first approximation of the structure of the Aurivillius phases mentioned earlier.

The crystal structure of $Bi_4Ti_3O_{12}$ has been studied by Dorrian *et al.* (1971). Their structure can be described as being derived from the space group *Fmmm* using irreducible representations of the electron density with effective space groups *Fmmm*, *F2mm*, *Bmab*, *Bbab* which Fourier transform to the real and imaginary components of $h + k$ even and $h + k$ odd data respectively. However, the *hk*0 reflections with *h* even, *k* odd are weakly present in electron diffraction data (Withers *et al.*, 1988) and the space group is *B1a1* as suggested by optical measurements (Dorrian *et al.*, 1971).

There are four further possible irreducible representations compatible with *B1a1* being a common subgroup of *Fmmm*. These correspond to *F*12/*m*1, *Fmm2*, *Bbam* and *Bmam*. The ferroelectricity shows *Fmm2* and *F2mm* are both present and the weak *hk*0 reflections show that at least one of *Bbam* and *Bmam* is present.

Table 4 selects from Table 2 the segmentation of structural information for the extra irreducible representations allowed by dropping crystal symmetry to *A1a1* or *B1a1*, which are the minimum symmetries compatible with the observed absence conditions. The four extra irreducible representations for the *A*-centred case correspond to *F*12/*m*1, *Fmm2*, *Abaa* and *Amaa*.

Implications for the identification of soft modes

The ability to define a displacive modulation with a particular irreducible representation depends on how well $F_p(\mathbf{h})$ can be obtained. Primarily, $|F(\mathbf{h})|^2 = |A(\mathbf{h})|^2 + |B(\mathbf{h})|^2$ is observed and information from a trial model can be used to obtain an estimate of $F(\mathbf{h})$ by saying that the phase $\exp(i\alpha_{\mathbf{h}}) = [A(\mathbf{h}) + iB(\mathbf{h})]/|F(\mathbf{h})|$ is the same for both calculated and observed data in order for least-squares refinement or the evaluation of scattering density to take place. If data is twinned so that $|Y(\mathbf{h})|^2 = \sum_q a_q |F(\mathbf{T}_q\mathbf{h})|^2$ is observed then estimates are made by saying $[A(\mathbf{h}) + iB(\mathbf{h})]/|Y(\mathbf{h})|$ is the same for both calculated and observed estimates.

If $A(\mathbf{h})$ is dominant over $B(\mathbf{h})$, then this procedure makes the discrepancies in $A(\mathbf{h})$ much bigger than the discrepancies in $B(\mathbf{h})$ when actually the goodness-of-fit statistics can accommodate larger discrepancies in $B(\mathbf{h})$ than in $A(\mathbf{h})$. The consequence of this is that false structure solutions can be obtained which are stable under refinement conditions.

The *eee* and *ooo* data are dominated by the parent structure. The existence of a large anomalous-

Table 2. *Functional forms for symmetrized displacements of isotropic atoms*

The geometric components of the structure factor for the symmetrized displacements of isotropic atoms on different equivalent positions are given. Equivalent positions related by *A* centring (or *B* centring) have been omitted. Only non-zero values and the associated index condition are listed. When $z = 0$ or $\frac{1}{4}$, zero contributions are implied systematically for the *l* index.

(*a*) Displacement of atoms from 0,0,*z*, *etc.* in the *Fmmm* parent structure

x coordinate

*F*12/*m*1	$\delta,0,z$	$-\delta,0,-z$	$\frac{1}{2}+\delta,\frac{1}{2},z$	$\frac{1}{2}-\delta,\frac{1}{2},-z$
*F*2*mm*	$\delta,0,z$	$\delta,0,-z$	$\frac{1}{2}+\delta,\frac{1}{2},z$	$\frac{1}{2}+\delta,\frac{1}{2},-z$
Abma (*Bbmb*)	$\delta,0,z$	$-\delta,0,-z$	$\frac{1}{2}-\delta,\frac{1}{2},z$	$\frac{1}{2}+\delta,\frac{1}{2},-z$
Abmm (*Bbmm*)	$\delta,0,z$	$\delta,0,-z$	$\frac{1}{2}-\delta,\frac{1}{2},z$	$\frac{1}{2}-\delta,\frac{1}{2},-z$

$h+k=2n$	$8\cos(2\pi lz)\cos(2\pi h\delta)$	*Fmmm*
	$-8\sin(2\pi lz)\sin(2\pi h\delta)$	*F*12/*m*1
	$8i\cos(2\pi lz)\sin(2\pi h\delta)$	*F*2*mm*
$h+k=2n+1$	$-8\sin(2\pi lz)\sin(2\pi h\delta)$	*Abma* (*Bbmb*)
	$8i\cos(2\pi lz)\sin(2\pi h\delta)$	*Abmm* (*Bbmm*)

y coordinate

*Fm*2*m*	$0,\delta,z$	$0,\delta,-z$	$\frac{1}{2},\frac{1}{2}+\delta,z$	$\frac{1}{2},\frac{1}{2}+\delta,-z$
*F*2/*m*11	$0,\delta,z$	$0,-\delta,-z$	$\frac{1}{2},\frac{1}{2}+\delta,z$	$\frac{1}{2},\frac{1}{2}-\delta,-z$
Amaa (*Bmab*)	$0,\delta,z$	$0,-\delta,-z$	$\frac{1}{2},\frac{1}{2}-\delta,z$	$\frac{1}{2},\frac{1}{2}+\delta,-z$
Amam (*Bmam*)	$0,\delta,z$	$0,\delta,-z$	$\frac{1}{2},\frac{1}{2}-\delta,z$	$\frac{1}{2},\frac{1}{2}-\delta,-z$

$h+k=2n$	$8\cos(2\pi lz)\cos(2\pi k\delta)$	*Fmmm*
	$-8\sin(2\pi lz)\sin(2\pi k\delta)$	*F*2/*m*11
	$8i\cos(2\pi lz)\sin(2\pi k\delta)$	*Fm*2*m*
$h+k=2n+1$	$-8\sin(2\pi lz)\sin(2\pi k\delta)$	*Amaa* (*Bmab*)
	$8i\cos(2\pi lz)\sin(2\pi k\delta)$	*Amam* (*Bmam*)

z coordinate

Fmmm	$0,0,z$	$0,0,-z$	$\frac{1}{2},\frac{1}{2},z$	$\frac{1}{2},\frac{1}{2},-z$
*Fmm*2	$0,0,z+\delta$	$0,0,-z+\delta$	$\frac{1}{2},\frac{1}{2},z+\delta$	$\frac{1}{2},\frac{1}{2},-z+\delta$
Ammm (*Bmmm*)	$0,0,z+\delta$	$0,0,-z-\delta$	$\frac{1}{2},\frac{1}{2},z-\delta$	$\frac{1}{2},\frac{1}{2},-z+\delta$
Amma (*Bmmb*)	$0,0,z+\delta$	$0,0,-z+\delta$	$\frac{1}{2},\frac{1}{2},z-\delta$	$\frac{1}{2},\frac{1}{2},-z-\delta$

$h+k=2n$	$8\cos(2\pi lz)\cos(2\pi l\delta)$	*Fmmm*
	$8i\cos(2\pi lz)\sin(2\pi l\delta)$	*Fmm*2
$h+k=2n+1$	$-8\sin(2\pi lz)\sin(2\pi l\delta)$	*Ammm* (*Bmmm*)
	$8i\cos(2\pi lz)\sin(2\pi l\delta)$	*Amma* (*Bmmb*)

(*b*) Displacement of atoms from $\frac{1}{4},\frac{1}{4},z$, *etc.* in the *Fmmm* parent structure

x coordinate

*F*2/*m*11	$\frac{1}{4}+\delta,\frac{1}{4},z$	$\frac{1}{4}-\delta,\frac{3}{4},z$	$\frac{3}{4}-\delta,\frac{1}{4},z$	$\frac{3}{4}+\delta,\frac{3}{4},z$
	$\frac{1}{4}-\delta,\frac{1}{4},-z$	$\frac{1}{4}+\delta,\frac{3}{4},-z$	$\frac{3}{4}+\delta,\frac{1}{4},z$	$\frac{3}{4}-\delta,\frac{3}{4},-z$
*Fm*2*m*	$\frac{1}{4}+\delta,\frac{1}{4},z$	$\frac{1}{4}-\delta,\frac{3}{4},z$	$\frac{3}{4}-\delta,\frac{1}{4},z$	$\frac{3}{4}+\delta,\frac{3}{4},z$
	$\frac{1}{4}+\delta,\frac{1}{4},-z$	$\frac{1}{4}-\delta,\frac{3}{4},-z$	$\frac{3}{4}-\delta,\frac{1}{4},-z$	$\frac{3}{4}+\delta,\frac{3}{4},-z$
*F*12/*m*1	$\frac{1}{4}+\delta,\frac{1}{4},z$	$\frac{1}{4}+\delta,\frac{3}{4},z$	$\frac{3}{4}+\delta,\frac{1}{4},z$	$\frac{3}{4}+\delta,\frac{3}{4},z$
	$\frac{1}{4}-\delta,\frac{1}{4},-z$	$\frac{1}{4}-\delta,\frac{3}{4},-z$	$\frac{3}{4}-\delta,\frac{1}{4},-z$	$\frac{3}{4}+\delta,\frac{3}{4},-z$
*F*2*mm*	$\frac{1}{4}+\delta,\frac{1}{4},z$	$\frac{1}{4}+\delta,\frac{3}{4},z$	$\frac{3}{4}+\delta,\frac{1}{4},z$	$\frac{3}{4}+\delta,\frac{3}{4},z$
	$\frac{1}{4}+\delta,\frac{1}{4},-z$	$\frac{1}{4}+\delta,\frac{3}{4},-z$	$\frac{3}{4}+\delta,\frac{1}{4},-z$	$\frac{3}{4}+\delta,\frac{3}{4},-z$
Aham (*Bbam*)	$\frac{1}{4}+\delta,\frac{1}{4},z$	$\frac{1}{4}-\delta,\frac{3}{4},z$	$\frac{3}{4}+\delta,\frac{1}{4},z$	$\frac{3}{4}-\delta,\frac{3}{4},z$
	$\frac{1}{4}+\delta,\frac{1}{4},-z$	$\frac{1}{4}-\delta,\frac{3}{4},-z$	$\frac{3}{4}+\delta,\frac{1}{4},-z$	$\frac{3}{4}-\delta,\frac{3}{4},-z$
Abaa (*Bbab*)	$\frac{1}{4}+\delta,\frac{1}{4},z$	$\frac{1}{4}-\delta,\frac{3}{4},z$	$\frac{3}{4}+\delta,\frac{1}{4},z$	$\frac{3}{4}-\delta,\frac{3}{4},z$
	$\frac{1}{4}-\delta,\frac{1}{4},-z$	$\frac{1}{4}+\delta,\frac{3}{4},-z$	$\frac{3}{4}-\delta,\frac{1}{4},-z$	$\frac{3}{4}+\delta,\frac{3}{4},-z$
Ammm (*Bmmm*)	$\frac{1}{4}+\delta,\frac{1}{4},z$	$\frac{1}{4}+\delta,\frac{3}{4},z$	$\frac{3}{4}-\delta,\frac{1}{4},z$	$\frac{3}{4}-\delta,\frac{3}{4},z$
	$\frac{1}{4}+\delta,\frac{1}{4},-z$	$\frac{1}{4}+\delta,\frac{3}{4},-z$	$\frac{3}{4}-\delta,\frac{1}{4},-z$	$\frac{3}{4}-\delta,\frac{3}{4},-z$
Amma (*Bmmb*)	$\frac{1}{4}+\delta,\frac{1}{4},z$	$\frac{1}{4}-\delta,\frac{3}{4},z$	$\frac{3}{4}-\delta,\frac{1}{4},z$	$\frac{3}{4}+\delta,\frac{3}{4},z$
	$\frac{1}{4}-\delta,\frac{1}{4},-z$	$\frac{1}{4}+\delta,\frac{3}{4},-z$	$\frac{3}{4}-\delta,\frac{1}{4},-z$	$\frac{3}{4}+\delta,\frac{3}{4},-z$

$h=2n,\ k=2n$	$16(-1)^{(h+k)/2}\cos(2\pi lz)\cos(2\pi h\delta)$	*Fmmm*
	$-16(-1)^{(h+k)/2}\sin(2\pi lz)\sin(2\pi h\delta)$	*F*12/*m*1
	$16i(-1)^{(h+k)/2}\cos(2\pi lz)\sin(2\pi h\delta)$	*F*2*mm*
$h=2n+1,\ k=2n+1$	$-16(-1)^{(h+k)/2}\sin(2\pi lz)\sin(2\pi h\delta)$	*F*2/*m*11
	$16i(-1)^{(h+k)/2}\cos(2\pi lz)\sin(2\pi h\delta)$	*Fm*2*m*
$h=2n,\ k=2n+1$	$-16\sin[2\pi(h+k)/4]\cos(2\pi lz)\sin(2\pi h\delta)$	*Abam* (*Bbam*)
	$-16i\sin[2\pi(h+k)/4]\sin(2\pi lz)\sin(2\pi h\delta)$	*Abaa* (*Bbab*)
$h=2n+1,\ k=2n$	$-16\sin[2\pi(h+k)/4)]\cos(2\pi lz)\sin(2\pi h\delta)$	*Ammm* (*Bmmm*)
	$-16i\sin[2\pi(h+k)/4]\sin(2\pi lz)\sin(2\pi h\delta)$	*Amma* (*Bmmb*)

y coordinate

*F*2/*m*11	$\frac{1}{4},\frac{1}{4}+\delta,z$	$\frac{1}{4},\frac{3}{4}+\delta,z$	$\frac{3}{4},\frac{1}{4}+\delta,z$	$\frac{3}{4},\frac{3}{4}+\delta,z$
	$\frac{1}{4},\frac{1}{4}-\delta,-z$	$\frac{1}{4},\frac{3}{4}-\delta,-z$	$\frac{3}{4},\frac{1}{4}-\delta,-z$	$\frac{3}{4},\frac{3}{4}-\delta,-z$
*Fm*2*m*	$\frac{1}{4},\frac{1}{4}+\delta,z$	$\frac{1}{4},\frac{3}{4}+\delta,z$	$\frac{3}{4},\frac{1}{4}+\delta,z$	$\frac{3}{4},\frac{3}{4}+\delta,z$
	$\frac{1}{4},\frac{1}{4}+\delta,-z$	$\frac{1}{4},\frac{3}{4}+\delta,-z$	$\frac{3}{4},\frac{1}{4}+\delta,-z$	$\frac{3}{4},\frac{3}{4}+\delta,-z$
*F*12/*m*1	$\frac{1}{4},\frac{1}{4}+\delta,z$	$\frac{1}{4},\frac{3}{4}-\delta,z$	$\frac{3}{4},\frac{1}{4}-\delta,z$	$\frac{3}{4},\frac{3}{4}+\delta,z$
	$\frac{1}{4},\frac{1}{4}-\delta,-z$	$\frac{1}{4},\frac{3}{4}+\delta,-z$	$\frac{3}{4},\frac{1}{4}+\delta,-z$	$\frac{3}{4},\frac{3}{4}-\delta,-z$
*F*2*mm*	$\frac{1}{4},\frac{1}{4}+\delta,z$	$\frac{1}{4},\frac{3}{4}-\delta,z$	$\frac{3}{4},\frac{1}{4}-\delta,z$	$\frac{3}{4},\frac{3}{4}+\delta,z$
	$\frac{1}{4},\frac{1}{4}+\delta,-z$	$\frac{1}{4},\frac{3}{4}-\delta,-z$	$\frac{3}{4},\frac{1}{4}+\delta,-z$	$\frac{3}{4},\frac{3}{4}+\delta,-z$
Abam (*Bbam*)	$\frac{1}{4},\frac{1}{4}+\delta,z$	$\frac{1}{4},\frac{3}{4}+\delta,z$	$\frac{3}{4},\frac{1}{4}-\delta,z$	$\frac{3}{4},\frac{3}{4}-\delta,z$
	$\frac{1}{4},\frac{1}{4}+\delta,-z$	$\frac{1}{4},\frac{3}{4}+\delta,-z$	$\frac{3}{4},\frac{1}{4}-\delta,-z$	$\frac{3}{4},\frac{3}{4}-\delta,-z$
Abaa (*Bbab*)	$\frac{1}{4},\frac{1}{4}+\delta,z$	$\frac{1}{4},\frac{3}{4}+\delta,z$	$\frac{3}{4},\frac{1}{4}-\delta,z$	$\frac{3}{4},\frac{3}{4}-\delta,z$
	$\frac{1}{4},\frac{1}{4}-\delta,-z$	$\frac{1}{4},\frac{3}{4}-\delta,-z$	$\frac{3}{4},\frac{1}{4}+\delta,-z$	$\frac{3}{4},\frac{3}{4}+\delta,-z$
Ammm (*Bmmm*)	$\frac{1}{4},\frac{1}{4}+\delta,z$	$\frac{1}{4},\frac{3}{4}-\delta,z$	$\frac{3}{4},\frac{1}{4}+\delta,z$	$\frac{3}{4},\frac{3}{4}-\delta,z$
	$\frac{1}{4},\frac{1}{4}+\delta,-z$	$\frac{1}{4},\frac{3}{4}-\delta,-z$	$\frac{3}{4},\frac{1}{4}+\delta,-z$	$\frac{3}{4},\frac{3}{4}-\delta,-z$
Amma (*Bmmb*)	$\frac{1}{4},\frac{1}{4}+\delta,z$	$\frac{1}{4},\frac{3}{4}-\delta,z$	$\frac{3}{4},\frac{1}{4}+\delta,z$	$\frac{3}{4},\frac{3}{4}-\delta,z$
	$\frac{1}{4},\frac{1}{4}-\delta,-z$	$\frac{1}{4},\frac{3}{4}+\delta,-z$	$\frac{3}{4},\frac{1}{4}-\delta1,-z$	$\frac{3}{4},\frac{3}{4}+\delta,-z$

$h=2n,\ k=2n$	$16(-1)^{(h+k)/2}\cos(2\pi lz)\cos(2\pi k\delta)$	*Fmmm*
	$-16(-1)^{(h+k)/2}\sin(2\pi lz)\sin(2\pi k\delta)$	*F*2/*m*11
	$16i(-1)^{(h+k)/2}\cos(2\pi lz)\sin(2\pi k\delta)$	*Fm*2*m*
$h=2n+1,\ k=2n+1$	$-16(-1)^{(h+k)/2}\sin(2\pi lz)\sin(2\pi k\delta)$	*F*12/*m*1
	$16i(-1)^{(h+k)/2}\cos(2\pi lz)\sin(2\pi k\delta)$	*F*2*mm*
$h=2n,\ k=2n+1$	$-16\sin[2\pi(h+k)/4]\cos(2\pi lz)\sin(2\pi k\delta)$	*Ammm* (*Bmmm*)
	$-16i\sin[2\pi(h+k)/4]\sin(2\pi lz)\sin(2\pi k\delta)$	*Amma* (*Bmmb*)
$h=2n+1,\ k=2n$	$-16\sin[2\pi(h+k)/4)]\cos(2\pi lz)\sin(2\pi k\delta)$	*Abam* (*Bbam*)
	$-16i\sin[2\pi(h+k)/4]\sin(2\pi lz)\sin(2\pi k\delta)$	*Abaa* (*Bbab*)

z coordinate

Fmmm	$\frac{1}{4},\frac{1}{4},z$	$\frac{1}{4},\frac{3}{4},z$	$\frac{3}{4},\frac{1}{4},z$	$\frac{3}{4},\frac{3}{4},z$
	$\frac{1}{4},\frac{1}{4},-z$	$\frac{1}{4},\frac{3}{4},-z$	$\frac{3}{4},\frac{1}{4},-z$	$\frac{3}{4},\frac{3}{4},-z$
*Fmm*2	$\frac{1}{4},\frac{1}{4},z+\delta$	$\frac{1}{4},\frac{3}{4},z+\delta$	$\frac{3}{4},\frac{1}{4},z+\delta$	$\frac{3}{4},\frac{3}{4},z+\delta$
	$\frac{1}{4},\frac{1}{4},-z+\delta$	$\frac{1}{4},\frac{3}{4},-z+\delta$	$\frac{3}{4},\frac{1}{4},-z+\delta$	$\frac{3}{4},\frac{3}{4},-z+\delta$
*F*112/*m*	$\frac{1}{4},\frac{1}{4},z+\delta$	$\frac{1}{4},\frac{3}{4},z-\delta$	$\frac{3}{4},\frac{1}{4},z-\delta$	$\frac{3}{4},\frac{3}{4},z+\delta$
	$\frac{1}{4},\frac{1}{4},-z-\delta$	$\frac{1}{4},\frac{3}{4},-z+\delta$	$\frac{3}{4},\frac{1}{4},-z+\delta$	$\frac{3}{4},\frac{3}{4},-z-\delta$
*F*222	$\frac{1}{4},\frac{1}{4},z+\delta$	$\frac{1}{4},\frac{3}{4},z-\delta$	$\frac{3}{4},\frac{1}{4},z-\delta$	$\frac{3}{4},\frac{3}{4},z+\delta$
	$\frac{1}{4},\frac{1}{4},-z+\delta$	$\frac{1}{4},\frac{3}{4},-z-\delta$	$\frac{3}{4},\frac{1}{4},-z-\delta$	$\frac{3}{4},\frac{3}{4},-z+\delta$
Abma (*Bbmb*)	$\frac{1}{4},\frac{1}{4},z+\delta$	$\frac{1}{4},\frac{3}{4},z+\delta$	$\frac{3}{4},\frac{1}{4},z-\delta$	$\frac{3}{4},\frac{3}{4},z-\delta$
	$\frac{1}{4},\frac{1}{4},-z+\delta$	$\frac{1}{4},\frac{3}{4},-z+\delta$	$\frac{3}{4},\frac{1}{4},-z+\delta$	$\frac{3}{4},\frac{3}{4},-z+\delta$
Abmm (*Bbmm*)	$\frac{1}{4},\frac{1}{4},z+\delta$	$\frac{1}{4},\frac{3}{4},z+\delta$	$\frac{3}{4},\frac{1}{4},z-\delta$	$\frac{3}{4},\frac{3}{4},z-\delta$
	$\frac{1}{4},\frac{1}{4},-z-\delta$	$\frac{1}{4},\frac{3}{4},-z-\delta$	$\frac{3}{4},\frac{1}{4},-z+\delta$	$\frac{3}{4},\frac{3}{4},-z+\delta$
Amaa (*Bmab*)	$\frac{1}{4},\frac{1}{4},z+\delta$	$\frac{1}{4},\frac{3}{4},z-\delta$	$\frac{3}{4},\frac{1}{4},z+\delta$	$\frac{3}{4},\frac{3}{4},z-\delta$
	$\frac{1}{4},\frac{1}{4},-z+\delta$	$\frac{1}{4},\frac{3}{4},-z-\delta$	$\frac{3}{4},\frac{1}{4},-z+\delta$	$\frac{3}{4},\frac{3}{4},-z-\delta$
Amam (*Bmam*)	$\frac{1}{4},\frac{1}{4},z+\delta$	$\frac{1}{4},\frac{3}{4},z-\delta$	$\frac{3}{4},\frac{1}{4},z+\delta$	$\frac{3}{4},\frac{3}{4},z-\delta$
	$\frac{1}{4},\frac{1}{4},-z-\delta$	$\frac{1}{4},\frac{3}{4},-z+\delta$	$\frac{3}{4},\frac{1}{4},-z-\delta$	$\frac{3}{4},\frac{3}{4},-z+\delta$

$h=2n,\ k=2n$	$16(-1)^{(h+k)/2}\cos(2\pi lz)\cos(2\pi l\delta)$	*Fmmm*
	$16i(-1)^{(h+k)/2}\cos(2\pi lz)\sin(2\pi l\delta)$	*Fmm*2
$h=2n+1,\ k=2n+1$	$-16(-1)^{(h+k)/2}\sin(2\pi lz)\sin(2\pi l\delta)$	*F*112/*m*
	$16i(-1)^{(h+k)/2}\cos(2\pi lz)\sin(2\pi l\delta)$	*F*222
$h=2n,\ k=2n+1$	$-16\sin[2\pi(h+k)/4]\cos(2\pi lz)\sin(2\pi l\delta)$	*Amaa* (*Bmab*)
	$-16i\sin[2\pi(h+k)/4]\sin(2\pi lz)\sin(2\pi l\delta)$	*Amam* (*Bmam*)
$h=2n+1,\ k=2n$	$-16\sin[2\pi(h+k)/4)]\cos(2\pi lz)\sin(2\pi l\delta)$	*Abma* (*Bbmb*)
	$-16i\sin[2\pi(h+k)/4]\sin(2\pi lz)\sin(2\pi l\delta)$	*Abmm* (*Bbmm*)

dispersion contribution of $\Delta f'' = 10{\cdot}559$ for Bi with Mo $K\alpha$ radiation allows a substantial contribution from $iB(\mathbf{h})$ to the observed data and distinguishes $F(hkl)$ from $F(\bar{h}\bar{k}\bar{l})$ data because of the breakdown of Friedel's law. However, it also dominates the imaginary contribution and, consequently, the phase of the individual *F*2*mm* contributions of other atoms will be very doubtful unless quality data, carefully corrected for absorption are used. The Ti atoms also show anomalous dispersion, $\Delta f'' = 0{\cdot}446$, and the *F*2*mm* displacement of these atoms produces a significant contribution to $A(\mathbf{h})$. However, the $\Delta f'' = 0{\cdot}008$ value for O is effectively zero. Large *x* displacements of O atoms that correlate with U_{11} thermal parameters are detectable in the *Fmmm* component of the scattering density, but the signs of these displacements can only be determined by the *Fmm*2 component at a stage of refinement when low *R* factors have already been obtained using an arbitrary phase for the displacement.

However, it should be noted that the magnitude of the derivatives of the structure factor with respect to displacements from the parent structures do not depend on the magnitude of the displacements to a

Table 3. *Distribution of first-order information for the atom displacements allowed in either $A2_1am$ or $B2ab$*

If a displacement exists in isolation there is an implied space-group symmetry. This imposes an index selection and a choice between a real and an imaginary contribution to the structure factor associated with the displacement. This assumes no anomalous dispersion in atomic scattering factors. (1) Refers to *eee* data, (2) refers to *ooo* data, (3) refers to either *eoo* (*A*) or *eoe* (*B*) data, and (4) refers to either *oee* (*A*) or *oeo* (*B*) data. Contributions are real for *Abam* and *Bmab*, and imaginary for *F2mm*, *Amam* and *Bbab*.

Special position in *Fmmm*		δx	δy	δz
0,0,*z*	8(*i*) *mm*2	*F*2*mm* (1), (2)	*Amam Bmab* (3), (4)	—
0,0,$\frac{1}{2}$	4(*b*) *mmm*	*F*2*mm* (1), (2)	*Amam* (3), (4)	
$\frac{1}{4},\frac{1}{4},z$	16(*j*) 2.	*F*2*mm* (1) *Abam Bbab* (3)	*F*2*mm* (2) *Abam Bbab* (4)	*Amam Bmab* (3)
$\frac{1}{4},\frac{1}{4},0$	8(*e*) 2/*m*.	*F*2*mm* (1) *Abam* (3)	*F*2*mm* (2) *Abam* (4)	*Bmab* (3)
$\frac{1}{4},\frac{1}{4},\frac{1}{4}$	8(*f*) 222	*F*2*mm* (1)	*Abam Bbab* (4)	*Amam Bmab* (3)

Table 4. *Distribution of first-order information for the atom displacements allowed by reducing $A2_1am$ or $B2ab$ symmetry to $A1a1$ or $B1a1$*

See comments in Table 3. Contributions are real for *F*12/*m*1, *Amaa* and *Bbam*, and imaginary for *Fmm*2, *Abaa* and *Bmam*.

Special position in *Fmmm*		δx	δy	δz
0,0,*z*	8(*i*) *mm*2	*F*12/*m*1 (1), (2)	*Amaa Bmam* (3), (4)	*Fmm*2 (1), (2)
0,0,$\frac{1}{2}$	4(*b*) *mmm*	—	*Bmam* (3), (4)	*Fmm*2 (1), (2)
$\frac{1}{4},\frac{1}{4},z$	16(*j*) 2.	*F*12/*m*1 (1)	*F*12/*m*1 (2)	*Fmm*2 (1)
		Abaa Bbam (3)	*Abaa Bbam* (4)	*Amaa Bmam* (3)
$\frac{1}{4},\frac{1}{4},0$	8(*e*) 2/*m*.	*Bbam* (3)	*Bbam* (4)	*Fmm*2 (1) *Amaa* (3)
$\frac{1}{4},\frac{1}{4},\frac{1}{4}$	8(*f*) 222	*Abaa Bbam* (3)	*F*12/*m*1 (2)	*Fmm*2 (1)

first approximation. Consequently, the reliability of all O-atom displacements will be similar in absolute terms, provided the signs of displacements are correct in order that $F(\mathbf{h})$ phase reliability is adequate.

It should also be noted that when displacement of an atom derives from more than one irreducible representation correlations occur in the expansion of $\exp(2\pi i\sum_m \mathbf{h}.\delta_m)$ describing the modification to the geometric term for an atom displaced by $\sum_m \delta_m$ from a special position in the parent structure. This is best seen by looking at terms involving $(\mathbf{h}.\delta_m)(\mathbf{h}.\delta_n)$ in the series expansion. The symmetry of the contribution of such a term is obtained by multiplying the irreducible representations for δ_m and δ_n. These correlations have the ability to resolve problems in the phase of displacements, especially when the displacements are large.

If the *F2mm* symmetry contribution to an atom's displacement is phased wrongly then this error will propagate into its correlation terms with the *Bbab* and *Bmab* contributions. If the *eoe* and *oeo* data is dominated by $A(\mathbf{h})$ (as it turns out to be) then the *Bmab* contribution is totally refinable, and this includes the correlation between the *F2mm* and *Bbab* contributions. Unfortunately, there is no *Bbab* first-order term for the site 8(*e*) $\frac{1}{4},\frac{1}{4},0$ and the phasing of the *F2mm* displacement from this site will depend totally on the quality of the *F*-centred data.

It is also unfortunate that if both the *F2mm* and the *Bbab* contributions to an atom's displacement are wrongly phased then the resulting correlation of *Bmab* symmetry will be correctly phased. Only O atoms contribute to the *Bbab* component which corresponds to $iB(\mathbf{h})$ for the *eoe* and *oeo* data. The implicit assumption of the least-squares refinement that calculated phases are correct means that the overall *Bbab* contribution cannot be incorrectly phased. What is more, even if the quality of *F*-centred data is sufficiently good to correctly phase an *F2mm* displacement, the assumed correctness of phase for *Bbab* may sufficiently restrain the refinement so as to maintain the initial model for the phase of the *F2mm* displacement.

However, the *y* displacement of a Bi atom can make a large contribution to *Bmab*. When this happens the consequence of anomalous dispersion is to put sufficient phase information into $iB(\mathbf{h})$ so as to correlate with the *Bmab* component. Consequently, even if the refinement is incapable of correcting the phase for a displacement, there will be sufficient information content to select the correct structure from the refinement statistics of the options.

When the symmetry is reduced to *B*1*a*1, the *F*12/*m*1 and *Bbam* contributions are readily resolved as they create differences between the magnitudes of the real components of *hkl* and $hk\bar{l}$ data. If the phases for large displacements associated with *B*2*ab* symmetry are correct, meaningful refinement of the *Fmm*2 and *Bmam* components should result from $(\mathbf{h}.\delta_m)(\mathbf{h}.\delta_n)$ correlations, *e.g.* *F2mm*Fmm2 = Bbab* Bmam = F*12/*m*1 and *Bbab*Fmm2 = F2mm*Bmam = Bbam*.

The possibility of partial twinning that overlaps *hkl* and $hk\bar{l}$ data is an extra complication. Twinning reduces the difference between the intensities of *hkl* and $hk\bar{l}$ data. In $Bi_4Ti_3O_{12}$ 90° twins are readily detectable by grain boundaries but a polarizing microscope is necessary to detect the other form of twinning. The fact that the crystals are plates perpendicular to **c*** only allows the guarantee that the crystal used for data collection had no 90° twinning and was not a 1:1 twin for *hkl* and $hk\bar{l}$ data.

If we define $F_1(hkl) = [F(hkl) + F(hk\bar{l})/2$ and $F_2(hkl) = [F(hkl) - F(hk\bar{l})]/2$ then $F_1(hkl)$ is the Fourier transform of the *Fmmm*, *F2mm*, *Bmab* and *Bbab* components of the scattering density and $F_2(hkl)$ is the Fourier transform of the *F*12/*m*1, *Fmm*2, *Bbam* and *Bmam* components. Now $(1-a)|F(hkl)|^2 + a|F(hk\bar{l})|^2 = |F_1(hkl)|^2 + |F_2(hkl)|^2 + (1-2a)[F_1(hkl)^*F_2(hkl) + F_1(hkl)F_2(hkl)^*]$. If twinning is ignored for data with $|F_1(hkl)| \gg |F_2(hkl)|$, then $F(hkl) = F_1(hkl) + F_2(hkl)$ will be substituted by $F_1(hkl) + (1-2a)F_2(hkl)$ to best fit observed data. This reduces the amplitude of the displacements associated with $F_2(hkl)$ by $(1-2a)$. However, data

that have $F_1(hkl)$ identically zero are observed as $|F_2(hkl)|^2$ and are not affected by twinning. This is the case for the $hk0$ pseudo-b-glide absences. The collection and monitoring of this data is an essential component of the refinement.

Use of anisotropic thermal parameters as an error diagnostic

If a refinement of $Bi_4Ti_3O_{12}$ is carried out using isotropic thermal parameters the tendency is for the refinement to be dominated by the centrosymmetric parts of the structure-factor calculation. Consider, for example, displacements from the position $\frac{1}{4},\frac{1}{4},z$ 16(j) 2_z in *Fmmm*. Reduction of the symmetry to *B2ab* creates two general positions $\frac{1}{4}+\Delta_1, \frac{1}{4}+\Delta_2, z+\Delta_3$ and $\frac{1}{4}+\Delta_4, \frac{3}{4}+\Delta_5, z-\Delta_3$, and displacements Δ can be decomposed into displacements δ_m of *F2mm*, *Bmab* and *Bbab* symmetry. The $(\mathbf{h}.\delta_m)(\mathbf{h}.\delta_n)$ correlations embodied in $\exp(2\pi i\sum_m \mathbf{h}.\delta_m)$ where $\mathbf{h} = h\mathbf{a}^* + k\mathbf{b}^* + l\mathbf{c}^*$ make the following contributions to the real components of the structure factor:

$$\begin{aligned} Fmmm &= F2mm^*F2mm + Bbab^*Bbab + Bmab^*Bmab \\ &\quad (+ \text{ for atom 1, } - \text{ for atom 2}) \\ &= [(\Delta_1^2+\Delta_4^2)/h^2 + (\Delta_2^2+\Delta_5^2)k^2 \\ &\quad \pm 2(\Delta_1\Delta_2 - \Delta_4\Delta_5)hk]/4 + \Delta_3^2 l^2 \\ Bmab &= Fmm2^*Bbab \ (+ \text{ for atom 1, } - \text{ for atom 2}) \\ &= \pm[(\Delta_1^2-\Delta_4^2)h^2 + (\Delta_2^2-\Delta_5^2)k^2 \\ &\quad \pm 2(\Delta_1\Delta_2 + \Delta_4\Delta_5)hk]/4. \end{aligned}$$

We note that only the hk contribution is sensitive to the phases of the Δ_i components. If isotropic atoms are used, $\Delta_1\Delta_2$ and $\Delta_4\Delta_5$ do not change sign during refinement. The real component of $h+k=2n$ data determines the parent structure and $(\Delta_1^2+\Delta_4^2)$, $(\Delta_2^2+\Delta_5^2)$ and Δ_3^2 while the real component of $h+k=2n+1$ data determines Δ_3 and that Δ_1^2 and Δ_2^2 belong to atom 1, while Δ_4^2 and Δ_5^2 belong to atom 2. If alternatives for $\Delta_1\Delta_2$ and $\Delta_4\Delta_5$ are tested using comparative isotropic refinements, then there are four independent sign combinations for each atom.

Functions $\exp(2\pi i\sum_m \mathbf{h}.\delta_m)$ and $\exp[-(2\pi\sum_m \mathbf{h}.\delta_m)^2/2]$ give identical terms for the $(\mathbf{h}.\delta_m)(\mathbf{h}.\delta_n)$ correlations. Consequently, if the atoms are held fixed at the positions obtained from isotropic refinement and anisotropic thermal parameters are then refined, the result will be that errors in $\Delta_1\Delta_2$ or $\Delta_4\Delta_5$ will be compensated for by the U_{12} thermal parameters of the respective atoms. This can be used as an error diagnostic and clearly distinguishes false minima.

If positional and anisotropic thermal parameters are refined simultaneously, positional parameters will tend to move so as to correct errors in $iB(hkl)$ and these movements will be compensated by changes in the thermal parameters so that the terms in $(\mathbf{h}.\delta_m)(\mathbf{h}.\delta_n)$ stay correct. However, the fourth-order term in $(\mathbf{h}.\delta_m)(\mathbf{h}.\delta_n)(\mathbf{h}.\delta_p)(\mathbf{h}.\delta_q)$ has a coefficient $(2\pi)^4/24$ for the positional term $\exp(2\pi i\sum_m \mathbf{h}.\delta_m)$ but $(2\pi)^4/8$ for the thermal term $\exp[-(2\pi\sum_m \mathbf{h}.\delta_m)^2/2]$. As a consequence, when displacements are sufficiently large the original displacements tend to be preserved and should there be no error in the hk term an error in model will only by detected by changing the signs of both the x and y displacements and running comparative refinements or by looking at the variation of occupancy between the two possible sites.

It was found that O(6) tended not to move when Δ_4 and Δ_5 were both wrongly phased because the displacement from $\frac{1}{4},\frac{1}{4},z$ is so large. However, O(5) moved from its position for isotropic refinement when Δ_1 and Δ_2 were both wrongly phased. We were unable to swap the phases of Δ_1 and Δ_2 of O(5) when either or both of these were wrong and Δ_4 and Δ_5 were both also wrong. However, if Δ_4 and Δ_5 describing O(6) are both correct O(5) will refine to the correct position. The ready correction of O(1) was probably because its displacement has no first-order *Bbab* component. Three unconstrained refinement cycles were necessary when O(1) to O(5) was corrected and nonpositive-definite thermal parameters featured in the first two cycles. The phase of the displacement was only corrected in the second cycle after large thermal parameters had been evaluated in the first cycle to compensate for an initial lesser atom movement. The third cycle reduced the anisotropy as the atom moved away from $\frac{1}{4},\frac{1}{4},z$.

One can conclude that a correct solution corresponds to an anisotropic refinement in which thermal parameters are small and there is minimum anisotropy. Also a check involving changing the sign of displacements for both x and y of an atom should make refinement parameters worse. The final solution we obtained satisfied these criteria. Misbehaved solutions exist with R factors only 1% higher. Thermal parameters also become more isotropic when the symmetry is reduced to *B1a1* and when twinning is taken into account.

Experimental

Polycrystalline specimens of $Bi_4Ti_3O_{12}$, $Bi_2BaNb_2O_9$, $Bi_2SrNb_2O_9$, $Bi_2SrTa_2O_9$ and Bi_3TiNbO_9 were prepared from > 99·9% purity starting materials. The appropriate oxides were used except for the alkaline-earth metals where carbonates were used. Stoichiometric mixtures of the appropriate ingredients were heated in open platinum crucibles with a final annealing temperature of 1373–1423 K. Single crystals of $Bi_4Ti_3O_{12}$ were grown according to the method described by Cummins & Cross (1968).

Reaction products were examined by X-ray powder diffraction (XRD) and electron diffraction. XRD patterns were recorded using a Guinier–Hagg camera with Cu $K\alpha_1$ radiation and Si as an internal standard (NBS standard No. 640). Refined unit-cell parameters are listed in Table 5. Electron diffraction patterns were recorded on Jeol 100CX and Philips EM430 transmission electron microscopes.

The crystal selected for X-ray diffraction data collection, after careful examination under a polarizing microscope, was considered to be free of 90° twinning and, as far as could be ascertained using a tilting stage, possessed no domains in which there were differing amounts of *c*-component polarization. The cut crystal approximated a square plate (0·210 × 0·210 × 0·015 mm) corresponding to approximate (110), ($\bar{1}$10), (001) reciprocal-space directions. Precise measurements of faces were made using the method devised by Alcock (1970). Dimensions used for the absorption correction were (001) 0·0073 (1), (00$\bar{1}$) 0·0073 (1), (102,82,$\bar{9}\bar{5}$) 0·136 (2), ($\bar{9}\bar{3}$,$\bar{8}\bar{5}$,$\bar{6}\bar{3}$) 0·080 (2), ($\bar{9}\bar{9}$,87,$\bar{7}\bar{6}$) 0·118 (2), (91,$\bar{9}\bar{2}$,82) 0·101 (2) mm. A full sphere of Mo $K\alpha$ data (5243 *B*-centred monochromator data) out to $\theta = 30°$ was recorded on a Philips four-circle automated diffractometer at 1° min^{-1} for a scan width of 1·3° with backgrounds of 15 s per side. The numerical absorption correction of *SHELX* (Sheldrick, 1976) chose 2610 grid points. The linear absorption coefficient μ(Mo $K\alpha$) was 747·3 cm^{-1} [856·6 cm^{-1} was used by Dorrian *et al.* (1971)]. Scattering curves, atomic absorption coefficients and anomalous-dispersion corrections were from *International Tables for X-ray Crystallography* (1974). The average *UB* matrix for data collection was

−0·009426	0·008097	0·021526
0·086406	0·098078	0·000035
−0·096901	0·086675	−0·002051

Absorption correction

Values of $-\ln A$ varied between 1·0 and 4·4. The consequence of the way the crystal was orientated relative to the goniometer was that the worst scenario for reflections related by *mmm* symmetry operations was that four had large values of $-\ln A$ while the other four did not. For example 4$\bar{4}$8, $\bar{4}\bar{4}$8, $\bar{4}$48, 44$\bar{8}$ have values of $-\ln A$ = 2·47, 2·49, 3·50, 3·52 while their 1*m*1 related counterparts 448, $\bar{4}\bar{4}$8, $\bar{4}$48, 44$\bar{8}$ had values of 1·21, 1·20, 1·21, 1·21. The members of a quartet were related by 112/*m* symmetry and the cut crystal approximates *mmm* symmetry. Had the crystal had exact *mmm* external symmetry and had the (001), (110) and (1$\bar{1}$0) faces been aligned with the goniometer axes with **c*** horizontal then the absorption correction would have had exact 112/*m* symmetry. The crystal was mounted close to this orientation and one readily sees the rapid change in large absorption corrections with orientation. Consequently, since the orientation matrix changed slightly during data collection, each absorption correction was made with the orientation matrix relevant at the time of collection. The 1*m*1 symmetry relating quartets of reflections with small and large $-\ln A$ corresponds to the correct diffraction symmetry for a properly corrected crystal.

As a requirement for the absorption-corrected data to be deemed usuable it was decided that the statistic for merging across this symmetry element had to be better than the statistic for merging for *m*11 symmetry and 11*m* symmetry. This was achieved by rejecting the small part of our data which was collected after a power failure interrupted collection and by optimizing the dimension of the thin direction of the crystal between the (001) and (00$\bar{1}$) faces by the evaluation of merge statistics between the truly equivalent *hkl* and *h*$\bar{k}$*l* reflections. These staticstics were subdivided into *eee*, *ooo*, *eoe* and *oeo* subsets so that potential agreement factors for refinement could be assessed.

Results of data merging

Overall values of $R_{\rm int} = \sum_{\mathbf{h}}\sum_i(|F(\mathbf{h}_i)|^2 - |F(\mathbf{h})|^2)/\sum_{\mathbf{h}}|F(\mathbf{h})|^2$ were calculated where $|F(\mathbf{h}_i)|^2$ is the *i*th observation of an equivalent or pseudoequivalent of the mean quantity $|F(\mathbf{h})|^2$. Assuming *mmm*, 2*mm* and 1*m*1 symmetry, values of 0·0492, 0·0245, 0·0220 respectively were obtained using all observed data collected before a power failure. This statistic does not downweight data with large absorption corrections. The removal of the 693 observed and unobserved data with $-\ln A > 2{\cdot}5$ reduced the values of *R* but only by about 0·001. A thickness of 0·0146 (2) mm was obtained for the thin dimension. This precision is not obtainable optically. A statistic that downweights data with large absorption corrections was also calculated. Values of $wR = [\sum_{\mathbf{h}}N_{\mathbf{h}}\sum_i w_{\mathbf{h}i} \times (|F(\mathbf{h}_i)| - |F(\mathbf{h})|)^2/\sum_{\mathbf{h}}(N_{\mathbf{h}}-1)\sum_i w_{\mathbf{h}i}|F(\mathbf{h})|^2]^{1/2}$, where $N_{\mathbf{h}}$ is the number of independent observations of $|F(\mathbf{h})|^2$, were obtained using *SHELX* and gave the following results for data of different index conditions.

Data used	*m*11	1*m*1	11*m*
All 3721 reflections	0·0370	0·0138	0·0180
(absorption uncorrected)	0·3067	0·1693	0·0908)
1006 *eee* reflections	0·0372	0·0147	0·0219
928 *ooo* reflections	0·0363	0·0124	0·0135
872 *eoe* reflections	0·0366	0·0128	0·0173
915 *oeo* reflections	0·0460	0·0131	0·0297

Selection of data

Because data with high $-\ln A$ were duplicated by equivalent data with low $-\ln A$ it was decided not to

Table 5. *Refined unit-cell parameters* (Å) *for some Aurivillius phases*

	a	*b*	*c*	Space group
$Bi_4Ti_3O_{12}$	5·450 (1)	5·4059 (6)	32·832 (3)	*B1a1*
$Bi_2BaNb_2O_9$	3·9334 (2)	3·9334 (2)	25·603 (2)	*I4/mmm*
$Bi_2SrNb_2O_9$	5·5094 (4)	5·5094 (4)	25·098 (3)	*A2$_1$am*
$Bi_2SrTa_2O_9$	5·5177 (5)	5·5177 (5)	25·040 (4)	*A2$_1$am*
Bi_3TiNbO_9	5·4398 (7)	5·3941 (7)	25·099 (5)	*A2$_1$am*

use any data with $-\ln A > 2{\cdot}5$. During refinement anisotropic secondary-extinction corrections were found to be necessary and as a consequence unmerged data were used since the correct evaluation of the anisotropy requires unmerged data. It was also decided not to modify weights from those imposed strictly by counting statistics. The adding of an arbitrary percentage error would have increased the relative weight of data with large absorption corrections compared to those with small corrections. Refinement used 3028 data. Of these 189 were considered to be unobserved [$I < 2\sigma(I)$] and were calculated solely to compare their statistics with the 5 *hk*0, *k* odd reflections considered to be definitely observed.

Refinement was monitored by segmenting data into seven categories (Table 8). Data for which $\sin\theta/\lambda < 0{\cdot}2$ Å^{-1} were isolated as being more intense and highlighting secondary-extinction effects. Data considered to be unobserved were also isolated. The remaining data were separated into four sets according to the *hkl* index conditions of Table 3. The observed *hk*0, *k* odd data were also isolated. These data are not affected by twinning because they contain contributions from only the *Bbam* and *Bmam* symmetry components of the scattering density.

Refinement of the structure of $Bi_4Ti_3O_{12}$

The initial model used isotropic thermal parameters for all atoms starting with the parameters of Dorrian *et al.* (1971) in space group *B*2*ab*. A check on Friedel's law gave a refinement cycle with a value for $R_1 = \sum_{\mathbf{h}}||F_{obs}(\mathbf{h})| - |F_{calc}(\mathbf{h})||/\sum_{\mathbf{h}}|F_{obs}(\mathbf{h})|$ of 0·062 compared with 0·094 for the incorrect polarity. No atoms moved substantially. Anisotropic refinement then followed and in three cycles the O(1) and O(4) atoms first went highly anisotropic, then changed the sign of their *x* displacements and then reduced anisotropy. Residual anisotropy consistent with a *Bbam* rotation of a TiO_6 octahedron was evident for O(1). The inclusion of this rotation reduces the symmetry to *B*1*a*1.

The segmentation of data clearly showed that secondary extinction was present. Data with $\sin\theta/\lambda < 0{\cdot}2$ Å^{-1} calculated substantially larger than observation on average while other data fitted well. An isotropic extinction correction could not reduce the value of R_1 for this data below 0·15 and so the anisotropic extinction parameterization described by Coppens & Hamilton (1970) was used. Type 2 extinction was preferred over type 1 because the resulting parameterization maintained crystal symmetry whereas the other option did not. In the final refinement cycle, data with $\sin\theta/\lambda < 0{\cdot}2$ Å^{-1} had a value for R_1 of 0·031. Removal of the extinction correction changed the scale of these 31 data so that $\sum_{\mathbf{h}}|F_{calc}(\mathbf{h})|/\sum_{\mathbf{h}}|F_{obs}(\mathbf{h})| = 1{\cdot}31$. Values of $W'_{11} = 10{\cdot}5\,(4)$, $W'_{22} = 0{\cdot}38\,(2)$, $W'_{33} = 5{\cdot}1\,(2)$ and $W'_{13} = -0{\cdot}1\,(3)$ were obtained. In type 2 extinction the reference direction is in the plane of the incoming and outgoing beams and at right angles to the incoming beam. At low angles this puts this direction almost coincident with the scattering vector **h**. The fact that the prinicpal axes of W' align with the crystal axes creates the observation that the extinction predominantly changes the mean intensity of reflections related by *mmm* symmetry and not differences between the reflections, as evidenced in the merge statistics obtained using raw data. The intense 020 reflection is the most affected and corresponds with the fact that W'_{22} is the smallest eigenvalue of W'.

Anisotropic refinement in space group *B*1*a*1 gave a final value for R_1 of 0·027 for the observed data and the positional parameters of model 2 in Table 6 with suspicious anisotropic thermal parameters for O(5) and O(5)′. Re-refining with isotropic atoms for O(5), O(5)′, O(6) and O(6)′ returned O(5) and O(5)′ towards the positions of Dorrian *et al.* and increased R_1 to 0·030. Projecting the amounts of each displacive mode it is seen that the signs of the *F*2*mm* and *Bbab* components for O(5) to O(6)′ do not change and that this sign is determined by the O(6) and O(6)′ atoms. Using the TiO_6 octahedron involving O(1) and O(1)′ as a model, a similar geometry could be obtained by changing the sign of the *x* and *y* displacements for the O(6) and O(6)′ atoms.

Anisotropic refinement of this model reduced R_1 to 0·020. Residual anisotropy was consistent with the *Bbam* mode being too small in amplitude as a result of twinning reducing the difference between $|F(hkl)|$ and $|F(hk\bar{l})|$ data. Isolation of the five *hk*0, *k* odd, reflections considered to be definitely observed showed that $k = \sum_{\mathbf{h}}|F_{calc}(\mathbf{h})|/\sum_{\mathbf{h}}|F_{obs}(\mathbf{h})|$ was only 0·21, while the value for the remaining unobserved data [$I < 2\sigma(I)$] was just over 1. A twin model was consequently refined to give a final R_1 of 0·0177 with $k = 0{\cdot}80$ for the five weak data and 1·11 for the 189 unobserved data.

A twin ratio of 0·629 (5):0·371 was obtained. The value of $(1 - 2\alpha) = 0{\cdot}258$ scales the difference between $|F(hkl)|$ and $|F(hk\bar{l})|$ data, see earlier, and results in U_{12} for the O(1) and O(1)′ atoms changing sign and becoming effectively zero (Table 7). The only constraints on the refinement, carried out using

Table 6. *Fractional coordinates for different refinements of* $Bi_4Ti_3O_{12}$

Model 1 gives the coordinates of Dorrian *et al.* (1971), model 2 gives the coordinates for a false minima at $R_1 = 0.027$ and model 3 gives the coordinates for the correct structure for which $R_1 = 0.018$. Fractional coordinates are multiplied by 10^4. Only model 3 included a twinning parameter.

	Model 1			Model 2			Model 3		
Bi(1)	0 (–)*	5022 (2)	5668 (0)	19 (1)	5023 (1)	5669 (1)	30 (1)	5023 (1)	5673 (1)
Bi(1)′	0 (–)*	4978 (2)	4332 (0)	15 (1)	4972 (1)	4333 (1)	13 (1)	4977 (1)	4336 (1)
Bi(2)	−9 (3)	4801 (1)	7114 (0)	−5 (1)*	4802 (1)	7113 (0)*	−21 (1)	4793 (1)	7113 (0)*
Bi(2)′	−9 (3)	5199 (1)	2886 (0)	5 (1)*	5195 (1)	2887 (0)*	21 (1)*	5185 (1)	2887 (0)*
Ti(1)	452 (8)	0 (–)	5000 (–)	432 (3)	−3 (9)	5002 (3)	446 (2)	−13 (6)	5007 (2)
Ti(2)	533 (6)	1 (1)	6286 (1)	501 (9)	1 (6)	6288 (3)	520 (6)	−4 (4)	6289 (2)
Ti(2)′	533 (6)	−1 (1)	3714 (1)	493 (9)	−3 (6)	3714 (3)	499 (6)	2 (4)	3717 (2)
O(1)	2070 (40)	2780 (50)	4967 (8)	3056 (18)	2588 (18)	5086 (5)	2990 (12)	2760 (12)	5102 (3)
O(1)′	2070 (40)	−2780 (50)	5033 (8)	3245 (17)	−2375 (17)	4934 (5)	3548 (11)	−2179 (11)	4942 (3)
O(2)	2640 (70)	2520 (90)	2501 (7)	2535 (24)	2570 (24)	2506 (9)	2704 (17)	2442 (16)	2495 (6)
O(2)′	2640 (70)	7480 (90)	7499 (7)	2537 (24)	7436 (24)	7494 (9)	2736 (16)	7571 (16)	7489 (6)
O(3)	730 (40)	250 (60)	5596 (8)	916 (27)	−652 (24)	5594 (6)	913 (18)	−705 (16)	5605 (4)
O(3)′	730 (40)	−250 (60)	4404 (8)	913 (27)	630 (24)	4415 (6)	918 (18)	587 (16)	4424 (4)
O(4)	−400 (40)	740 (50)	6815 (8)	553 (36)	508 (29)	6816 (8)	552 (24)	584 (19)	6825 (5)
O(4)′	−400 (40)	−740 (50)	3185 (8)	555 (36)	−501 (29)	3191 (8)	568 (24)	−441 (19)	3195 (5)
O(5)	2940 (40)	2150 (60)	6215 (8)	2469 (27)	2544 (23)	6118 (8)	2904 (18)	2800 (15)	6121 (5)
O(5)′	2940 (40)	−2150 (60)	3785 (8)	2480 (27)	−2517 (23)	3881 (8)	2962 (18)	−2659 (16)	3892 (5)
O(6)	1590 (40)	−3000 (50)	6310 (8)	1510 (25)	−2945 (23)	6227 (8)	3677 (17)	−1959 (15)	6244 (4)
O(6)′	1590 (40)	3000 (50)	3690 (8)	1465 (25)	2980 (23)	3770 (8)	3496 (17)	2164 (15)	3773 (4)

* These coordinates were constrained to define the origin.

Table 7. *U_{ij} thermal parameters for* $Bi_4Ti_3O_{12}$

The thermal parameters of atoms X and X' related by the pseudo-2_x symmetry axis were constrained so that $U_{ij} = U_{ij}'$ for ij = 11, 22, 33, 23 and $U_{ij} = -U_{ij}'$ for ij = 12, 13. Values are $\times 10^{-3}$ Å^2.

	U_{11}	U_{22}	U_{33}	U_{12}	U_{13}	U_{23}	$\langle U \rangle$
Bi(1)	8 (0)	10 (0)	12 (0)	0 (0)	3 (0)	0 (0)	10 (0)
Bi(2)	11 (0)	9 (0)	10 (0)	0 (0)	2 (0)	2 (0)	10 (0)
Ti(1)	6 (1)	5 (0)	9 (1)	0 (–)	0 (–)	0 (0)	7 (0)
Ti(2)	5 (0)	5 (0)	7 (0)	0 (0)	1 (0)	0 (0)	6 (0)
O(1)	6 (2)	7 (2)	14 (3)	2 (2)	3 (2)	1 (2)	9 (1)
O(2)	9 (2)	7 (1)	5 (2)	0 (1)	−2 (2)	−1 (2)	7 (1)
O(3)	10 (1)	10 (1)	12 (2)	−1 (2)	0 (2)	1 (2)	10 (1)
O(4)	20 (2)	13 (1)	6 (2)	3 (1)	−2 (1)	−4 (1)	13 (1)
O(5)	7 (2)	7 (1)	12 (3)	0 (1)	0 (2)	0 (1)	8 (1)
O(6)	7 (2)	5 (1)	16 (3)	2 (1)	1 (2)	0 (1)	9 (1)

Table 8. *Final refinement statistics for* $Bi_4Ti_3O_{12}$

Data set	R_1	wR	G.o.f.
All 2839 observed data	0·0177	0·0199	1·33
(1) 827 *eee* data	0·0160	0·0210	1·63
(2) 742 *ooo* data	0·0151	0·0176	1·36
(3) 618 *eoe* data	0·0240	0·0196	1·01
(4) 616 *oeo* data	0·0229	0·0186	1·02
(5) 5 *hk*0, *k* odd data	0·226	0·224	2·06
(6) 31 $\sin\theta/\lambda < 0.2$ Å^{-1} data	0·0311	0·0292	2·50
(7) 189 $I > 2\sigma(I)$ data	0·370	0·349	0·79

Notes: $R_1 = \sum_h ||F_{obs}(\mathbf{h})| - |F_{calc}(\mathbf{h})|| / \sum_h |F_{obs}(\mathbf{h})|$, $wR = [\sum_h w_h (|F_{obs}(\mathbf{h})| - |F_{calc}(\mathbf{h})|)^2 / \sum_h w_h |F_{obs}(\mathbf{h})|^2]^{1/2}$, G.o.f. $= [\sum_h w_h (|F_{obs}(\mathbf{h})| - |F_{calc}(\mathbf{h})|)^2 / (n-m)]^{1/2}$.

the program *RAELS* (Rae, 1989), came from using the twofold symmetry implicit in *B2ab* to relate thermal parameters of atoms related by the pseudo-symmetry. To fix the origin, the Bi(2) and Bi(2)′ atoms were constrained to make their displacive contributions to *F2mm* and *Fmm2* be zero.

The final minimum obtained was thoroughly tested, and can be relied upon because of the small thermal parameters and similarities in Ti environments. Considerations in assessing the quality of the answer were elaborated earlier. Analysis of the refinement from possible false minima was also summarized. Refinement statistics for the final cycle are given in Table 8.*

Description of the structure

The decomposition of the final structure in terms of displacements associated with different irreducible representations is given in Table 9. Interatomic distances are given in Table 10. The structure is substantially different from that of Dorrian *et al.* (1971), especially in terms of the *F2mm* component and the omitted *Bbam* and *Fmm2* components. It is reasonable to suspect that the displacive modes that exist in the structure of $Bi_3(Ti,Nb)O_9$ will be similar to those in this structure, but with the central octahedron removed and O(3) and O(3)′ coalesced. We intend to redetermine this structure and will extensively discuss the crystal chemistry of Aurivillius phases at that time.

Fig. 2 shows the *Bmab* component of the atom displacements. This motion can be described as a soft mode in which TiO_6 octahedra rotate about axes parallel to the polar direction **a** with alternating signs for the rotation as z increases. Ignoring the centring, this mode has *man* symmetry when an odd number of perovskite layers exists, $n = 3$ for $Bi_4Ti_3O_{12}$, but *mam* symmetry when an even number of perovskite layers exist, $n = 2$ for $Bi_3(Ti,Nb)O_9$. The imposition of 2_1ab symmetry across the Bi_2O_2 layer then generates space groups *B2ab* for $n = 3$ and $A2_1ab$ for $n = 2$.

The coexistence of the polar *F2mm* displacement and the Bmab (or *Amam* for $n = 2$) displacement

* A list of structure factors has been deposited with the British Library Document Supply Centre as Supplementary Publication No. SUP 52786 (20 pp.). Copies may be obtained through The Technical Editor, International Union of Crystallography, 5 Abbey Square, Chester CH1 2HU, England.

Table 9. *Displacements for modulation modes of* $Bi_4Ti_3O_{12}$

Values are listed × 10^3 Å.

	F2mm		*Bmab*		*Bbab*		*F*12/*m*1		*Fmm*2	*Bbam*		*Bmam*	
	δX	δY	δY	δZ	δX	δY	δX	δY	δZ	δX	δY	δY	δZ
Bi(1)	12		12				5		15			0	
Bi(1)′	12		−12				−5		15			0	
Bi(2)	0*		−106				−12		0*			−6	
Bi(2)′	0*		106				12		0*			−6	
Ti(1)	243								24			−7	
Ti(2)	277		−1				5		9			0	
Ti(2)′	277		1				−5		9			0	
O(1)	419	−17		262					71	−152	157		
O(1)′	419	17		−262					71	152	157		
O(2)	119			10		−35		3	−27	−8			
O(2)′	119			−10		35		3	−27	8			
O(3)	499		−349				−1		47			−31	
O(3)′	499		349				1		47			−31	
O(4)	305		277				−4		32			38	
O(4)′	305		−277				4		32			38	
O(5)	414	−56		−199	−178	180	16	−8	24	−34	47		−3
O(5)′	414	56		199	−178	−180	−16	−8	24	34	47		−3
O(6)	414	56		199	178	180	16	8	24	34	47		3
O(6)′	414	−56		−199	178	−180	−16	8	24	−34	47		3

* These displacements have zero values as they were used to fix the origin in *B*1*a*1. The sum of the atomic displacements from each mode equals the displacements obtained by least-squares refinement.

Table 10. *Geometry of the* Ti *and* Bi *environments in* $Bi_4Ti_3O_{12}$

Distances (Å)

Only distances < 3·5 Å are listed. Distances in the same row of the table would be equivalent in the *Fmmm* parent structure. O atoms are coded to indicate which special position of *Fmmm* they are displaced from, namely: (i) $\frac{1}{4}, \frac{1}{4}, z$; (ii) $-\frac{1}{4}, \frac{1}{4}, z$; (iii) $\frac{1}{4}, \frac{3}{4}, z$; (iv) $-\frac{1}{4}, \frac{3}{4}, z$; (v) $\frac{1}{4}, -\frac{1}{4}, z$; (vi) $-\frac{1}{4}, -\frac{1}{4}, z$ and (vii) 0, 0, *z*; (viii) 0, 1, *z*; (ix) $\frac{1}{2}, \frac{1}{2}, z$; (x) $-\frac{1}{2}, \frac{1}{2}, z$ respectively.

Bi(1)	—O(1′)	2·759 (9)	—O(1^{ii})	2·648 (9)	—O(1^{iii})′	3·424 (8)	—O(1^{iv})′	2·787 (9)
	—O(3^{vii})	3·141 (9)	—O(3^{viii})	2·370 (9)	—O(3^{ix})	3·235 (10)	—O(3^{x})	2·285 (10)
	—O(5′)	2·462 (12)	—O(5^{ii})	2·416 (12)	—O(6^{iii})	3·183 (11)	—O(6^{iv})	2·271 (12)
Bi(1)′	—O(1′)	3·222 (9)	—O(1^{ii})	3·118 (9)	—O(1^{iii})′	3·167 (8)	—O(1^{iv})′	2·451 (9)
	—O(3^{vii})′	2·441 (9)	—O(3^{viii})′	3·087 (9)	—O(3^{ix})′	3·246 (10)	—O(3^{x})′	2·271 (10)
	—O(6)′	3·056 (11)	—O(6^{ii})′	2·334 (12)	—O(5^{iii})′	2·520 (12)	—O(5^{iv})′	2·342 (13)
Bi(2)	—O(2′)	2·289 (13)	—O(2^{ii})	2·174 (14)	—O(2^{iii})′	2·457 (12)	—O(2^{iv})′	2·247 (13)
	—O(4^{vii})	2·483 (11)	—O(4^{viii})	3·285 (11)	—O(4^{ix})	3·188 (13)	—O(4^{x})	2·599 (14)
	—O(6^{iv})	3·164 (12)						
Bi(2)′	—O(2′)	2·449 (13)	—O(2^{ii})	2·296 (13)	—O(2^{iii})′	2·318 (13)	—O(2^{iv})′	2·219 (14)
	—O(4^{vii})′	3·219 (11)	—O(4^{viii})′	2·588 (11)	—O(4^{ix})′	3·191 (13)	—O(4^{x})′	2·632 (14)
	—O(6^{ii})′	3·280 (12)						
Ti(1)	—O(1′)	2·067 (7)	—O(1^{ii})	1·836 (7)	—O(1^{v})′	2·067 (6)	—O(1^{vi})′	1·850 (7)
	—O(3^{vii})	2·013 (14)	—O(3^{viii})′	1·959 (14)				
Ti(2)	—O(5′)	2·071 (10)	—O(5^{ii})	1·938 (10)	—O(6^{v})	2·025 (9)	—O(6^{vi})	1·931 (9)
	—O(3^{vii})	2·289 (15)						
	—O(4^{vii})	1·788 (18)						
Ti(2)′	—O(6)′	2·017 (9)	—O(6^{ii})′	1·890 (9)	—O(5^{v})′	2·050 (10)	—O(5^{vi})′	1·961 (11)
	—O(3^{vii})′	2·356 (15)						
	—O(4^{viii})′	1·730 (18)						

Angles (°)

O(1′)—Ti(1)—O(1^{vi})′	171·4 (3)	O(1^{ii})—Ti(1)—O(1^{v})′	171·6 (4)	O(3^{viii})—Ti(1)—O(3^{viii})′	165·1 (2)
O(5′)—Ti(2)—O(6^{vi})	158·2 (6)	O(5^{ii})—Ti(2)—O(6^{v})′	157·7 (6)	O(3^{vii})—Ti(2)—O(4^{viii})	174·0 (5)
O(5′)′—Ti(2)′—O(6^{ii})′	156·9 (7)	O(5^{vi})′—Ti(2)′—O(6)′	156·7 (6)	O(3^{viii})′—Ti(2)′—O(4^{viii})′	173·2 (5)

implies the possible coexistence of a *Bbab* (or *Abam*) displacement. The *F2mm* mode is shown in Fig. 3. The extra mode corresponds to rotations of TiO_6 octahedra about axes parallel to **c**. Looking down **c**, these rotations are in the same sense for $n = 2$ because of mirror symmetry, but an antimirror symmetry exists for *Bbab*. Thus the central Ti(1)O_6 octahedron in $Bi_4Ti_3O_{12}$ shows no rotation in this mode. The rotation of the Ti(2)O_6 octahedron is shown in Fig. 4.

Rotation of the central Ti(1)O_6 octahedron about **c** requires a mode of *Bbam* symmetry. The *F2mm* and *Bmab* modes have the largest displacements but those for the *Bbab* and *Bbam* modes are almost as large. The angular displacements are 7·5, 0, −7·5° for the *Bbab* mode and 1·7, 6·5, 1·7° for the *Bbam* mode. The resulting angles, namely 9·2, 6·5, −5·8°, suggest these rotations are involved with a unit-cell volume reduction. The residual anisotropy of thermal motions in Table 7 is consistent with extra low-frequency rotations of the TiO_6 octahedra about axes perpendicular to **c**.

The remaining *F*12/*m*1, *Fmm*2 and *Bmam* modes have smaller displacive amplitudes and would appear to be induced. The magnitudes of these modes and of the *Bbam* mode depend on the twin ratio and could be too small by up to 30%. Large errors also result because twinning reduced the difference between *hkl*

and $hk\bar{l}$ data. The optically observed polar *Fmm*2 displacement would be induced by the symmetry product *Bbam***Bbab* which couples the rotations about **c**. The *F*12/*m*1 mode would come from *Bbam** *Bmab* and the *Bmam* mode from *Bbam***F*2*mm*.

The implied imposition of 2_1ab symmetry across the $Bi(2)_2O(2)_2$ layer is manifested in the substantial *F*2*mm* and *Bmab* components for the O(2), Bi(2) and O(4) atoms. The only *Bbab* component for any of these atoms is small, −0·035 Å, and is associated with the *y* of O(2). This supports our proposition that the *F*2*mm* and *Bmab* (or *Amam*) modes are the important ones for conveying coherence between slabs of perovskite separated along **c**. Analysis of the Bi-atom displacement relative to the four O(2) atoms which would be equidistant for *Fmmm* symmetry shows that the Bi(2) moves preferentially towards one of the O(2) atoms, shortening one bond, leaving the two adjacent Bi(2)—O(2) bonds unchanged and lengthening the other. The 2_1ab symmetry gives a maximum separation between the shorter (also longer) bonds in the Bi_2O_2 layer.

We have calculated the dipole moments using ionic species Bi^{3+}, Ti^{4+}, O^{2-} and obtained values of 36·3 and 2·4 $\mu C\,cm^{-2}$ for the *x* and *z* components, which agrees well with the experimental results of Cross & Pohanka (1971). We see from Table 9 that all Ti and O atoms move a substantial amount in the *x* direction relative to the Bi atoms (not the case in the description of Dorrian *et al.*). However, the Ti atoms do not move as far as do the octahedra of O atoms surrounding them. The O(2) atoms which are part of the Bi_2O_2 layer move less than the other O and Ti atoms.

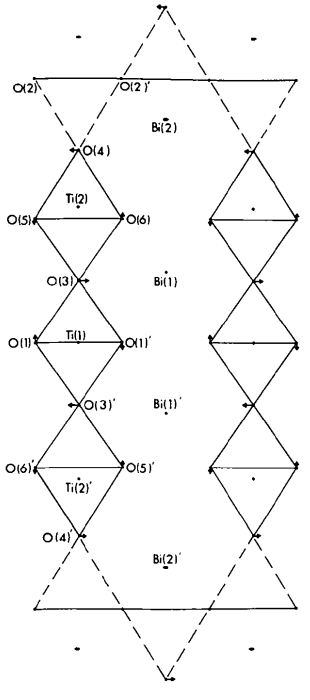

Fig. 2. A section of the *Fmmm* parent structure projected down **a**. The superimposed arrows correspond to the *Bmab* component of the atom displacements (see Table 8). The other section per unit cell is displaced by (**a** + **b**)/2 and is not shown. The arrows are reversed for this other section. Only atoms between $\frac{1}{4}$**c** and $\frac{3}{4}$**c** are shown. The remaining atoms are related by *B* centring.

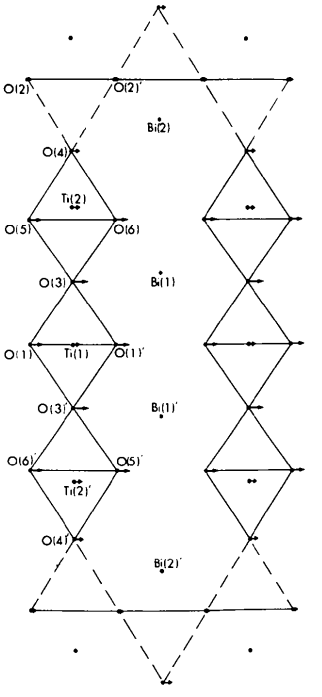

Fig. 3. A section of the *Fmmm* parent structure projected down **b**. The superimposed arrows correspond to the *F*2*mm* component of the atom displacements (see Table 9). The other section per unit cell is displaced by (**a** + **b**)/2 and is not shown. Only atoms between $\frac{1}{4}$ and $\frac{3}{4}$ are shown. The remaining atoms are related by *B* centring. The *F*2*mm* component corresponds to the spontaneous polarization along **a**.

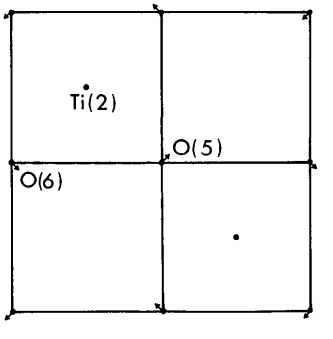

Fig. 4. The *Bbab* displacive mode showing the rotation of $Ti(2)O_6$ octahedra about the *c* axis. The $Ti(2)'O_6$ octahedra have an equal but opposite rotation. $Ti(1)O_6$ octahedra have no *Bbab* component.

It is seen that a first-order description of the structure includes an *F2mm* displacement of the TiO_6 octahedra relative to the remaining atoms rather than a movement of Ti atoms relative to their surrounding O atoms. This produces a larger dipole moment than is the case for many other Aurivillius phases and is probably induced by the lone pair of electrons on each Bi^{3+} ion. The structure shows a substantial spread in Bi—O distances that would have been equal for zero displacements from the *Fmmm* parent structure. Distances are given in Table 10. The Ti—O distances are more equal but the Ti atoms do not lie at the centres of mass of their surrounding O octahedra. Deviations of O—Ti—O angles from 180° for opposed O atoms are included in Table 10. The large *z* displacement components of Ti(2) and Ti(2)′ are such as to increase their distance from Ti(1).

In the parent structure each Bi atom is at $0,\frac{1}{2},z$ and is surrounded by O atoms at about the same *z* height at (vii) 0,0,*z*; (viii) 0,1,*z*; (ix) $\frac{1}{2},\frac{1}{2},z$; (x) $-\frac{1}{2},\frac{1}{2},z$ at distances of about 2·7 Å. It is seen that the *Fmm*2 mode (Fig. 3) reduces the Bi—O^{x} distances at the expense of Bi—O^{ix} distances and that the *Bmab* mode (Fig. 2) shortens one and lengthens the other of the pairs of Bi—O^{vii} and Bi—O^{viii} distances in an alternating pattern for the sequence Bi(2)′, Bi(1)′, Bi(1), Bi(2). The Bi(2) and Bi(2)′ atoms have a 0·106 Å *Bmab* displacement that assists the bond-length reduction of the shorter bond. The *Bbam* rotations of the $Ti(1)O_6$ octahedron cause the Bi(1) and Bi(1)′ environments to be quite different. This is highlighted in the first four distances tabulated for each atom. All Bi environments are highly asymmetric as is expected since each Bi^{3+} ion has a lone pair of electrons.

The authors wish to thank Dr J. D. FitzGerald for assistance with optical microscopy and Dr N. W. Alcock for assistance with crystal measurement.

References

ALCOCK, N. W. (1970). *Acta Cryst.* A**26**, 437–439.

AURIVILLIUS, B. (1949). *Ark. Kemi*, **1**, 463–480.

AURIVILLIUS, B. (1950). *Ark. Kemi*, **2**, 519–527.

BRADLEY, C. J. & CRACKNELL, A. P. (1972). *The Mathematical Theory of Symmetry in Solids. Representation Theory for Point Groups and Space Groups.* Oxford: Clarendon Press.

COPPENS, P. & HAMILTON, W. C. (1970). *Acta Cryst.* A**26**, 71–83.

CROSS, L. E. & POHANKA, R. C. (1971). *Mater. Res. Bull.* **6**, 939–950.

CUMMINS, S. E. & CROSS, L. E. (1968). *J. Appl. Phys.* **39**, 2268–2274.

DORRIAN, J. F., NEWNHAM, R. E., SMITH, T. K. & KAY, M. I. (1971). *Ferroelectrics*, **3**, 17–27.

International Tables for X-ray Crystallography (1974). Vol IV. Birmingham: Kynoch Press. (Present distributor Kluwer Academic Publishers, Dordrecht.)

MCCONNELL, J. D. C. & HEINE, V. (1984). *Acta Cryst.* A**40**, 473–482.

NEWNHAM, R. E., WOLFE, R. W. & DORRIAN, J. F. (1971). *Mater. Res. Bull.* **6**, 1029–1040.

NEWNHAM, R. E., WOLFE, R. W., HORSEY, R. S., DIAZ-COLON, F. A. & KAY, M. I. (1973). *Mater. Res. Bull.* **8**, 1183–1195.

RAE, A. D. (1989). *RAELS*89. *A Comprehensive Constrained Least-Squares Refinement Program.* Univ. of New South Wales, Australia.

SHELDRICK, G. M. (1976). *SHELX*76. Program for crystal structure determination. Univ. of Cambridge, England.

SINGH, K., BOPARDIKAR, D. K. & ATKARE, D. V. (1988). *Ferroelectrics*, **82**, 55–67.

SUBBARAO, E. C. (1973). *Ferroelectrics*, **5**, 267–280.

WITHERS, R. L. THOMPSON, J. G., WALLENBERG, I. R., FITZGERALD, J. D., ANDERSON, J. S. & HYDE, B. G. (1988). *J. Phys. C*, **21**, 6067–6083.

WOLFE, R. W., NEWNHAM, R. E. & KAY, M. I. (1969). *Solid State Commun.* **7**, 1797–1801.

WOLFE, R. W., NEWNHAM, R. E., SMITH, T. K. & KAY, M. I. (1971). *Ferroelectrics*, **3**, 1–7.

Acta Cryst. (1990). B**46**, 487–492

Structure of the Incommensurate Composite Crystal $(PbS)_{1\cdot12}VS_2$

BY MITSUKO ONODA AND KATSUO KATO

National Institute for Research in Inorganic Materials, 1-1 *Namiki, Tsukuba, Ibaraki* 305, *Japan*

AND YOSHITO GOTOH AND YOSHINAO OOSAWA

National Chemical Laboratory for Industry, 1-1 *Higashi, Tsukuba, Ibaraki* 305, *Japan*

(*Received* 2 *November* 1989; *accepted* 20 *March* 1990)

Abstract

The structure of the incommensurate composite crystal of the monoclinic layered sulfide $(PbS)_{1\cdot12}VS_2$, M_r = 384·20, has been analyzed on the basis of a four-dimensional superspace group. The crystal is composed of alternately stacked two-atom-thick PbS layers with a distorted NaCl-type structure, and VS_2 sandwiches with a distorted CdI_2-type structure. For 1780 unique reflections measured by single-crystal

0108-7681/90/040487-06$03.00